Progress In Electromagnetics Research B, Vol. 87, 151–170, 2020

Waveguide Radiation of the Combined Vibrator-Slot Structures

Sergey L. Berdnik, Victor A. Katrich, Mikhail V. Nesterenko*, and Yuriy M. Penkin

Abstract—A problem of electromagnetic wave diffraction by a longitudinal slot cut in a waveguide wide wall is solved by a generalized method of induced electro-magneto-motive forces (EMMF). The slot radiates in a half-space above a perfectly conducting plane where two vertical impedance monopoles are arbitrarily located. To control electrodynamic characteristics of the radiator, a passive impedance monopole is placed in the waveguide. The paper is aimed at the study of the electrodynamic characteristics of waveguide vibrator-slot structures, analogous to the known Clavin element, with two identical impedance monopoles on both sides of the narrow half-wave slot. The influence of the geometric structure parameters on the directional characteristic of Clavin type element: relative level of sidelobes in the E-plane and the RP width differences in the main polarization plane at -3 dB level was analyzed. It was shown that the directional and energy characteristics of the radiators: radiation and reflection coefficients, antenna directivity, and gain can be varied within wide limits by changing the electrical length and/or distributed surface impedance of the vibrators.

1. INTRODUCTION

In the modern practice, slotted structures are used as stand-alone small-sized antennas, elements of complex antenna arrays, and devices of antenna-feeder tracts [1–3]. To excite slot radiators and control their electrodynamic characteristics, vibrator-type elements are often used [4]. In combined vibrator-slot structures, the vibrator elements can have a different configuration and can be located in any electrodynamic volume coupling through a slot. For example, structures consisting of wire radiators located over an infinite perfectly conducting plane with a hole radiating into half space over a plane were considered in [5–10]. Radiators with vibrators located in various waveguide tracts and resonators were studied in [11–20]. A special place among combined vibrator-slot structures is occupied by Clavin elements, consisting of narrow radiating slot and two identical passive vibrators (monopoles) located on both sides of the slot cut in plane screen [21–28]. The Clavin element is characterized by similar radiation patterns (RPs) in the E- and H-planes. They are used as stand-alone radiators, primary feed antennas, and also as part of multi-element phased arrays [28]. However, in publications on this subject by other authors [11–16, 21–25], only perfectly conducting vibrators were considered. New possibilities for controlling the characteristics of vibrator-slot radiating structures by using monopoles with distributed surface impedance were proposed in [3, 4, 17–20, 26, 27].

In this paper, the excitation of electromagnetic fields by the combined radiator consisting of a longitudinal slot cut in a broad wall of the rectangular waveguide and vertical impedance monopoles is solved by the generalized method of induced EMMF [1, 3, 4, 29]. The dimensions of the impedance monopoles and their locations in space above the plane are arbitrary. The electrodynamic characteristics of the combined radiator can also be controlled by a passive impedance monopole located in the waveguide. The radiation characteristics of vibrator-slot structures similar to the Clavin element are thoroughly studied.

Received 28 May 2020, Accepted 7 July 2020, Scheduled 4 August 2020

* Corresponding author: Mikhail V. Nesterenko (mikhail.v.nesterenko@gmail.com).

The authors are with the Department of Radiophysics, Biomedical Electronics and Computer Systems, V. N. Karazin Kharkiv National University, 4, Svobody Sq., Kharkiv 61022, Ukraine.

2. PROBLEM FORMULATION AND INITIAL EQUATIONS IN THE GENERAL CASE

Consider a microwave device consisting of a rectangular waveguide section with a longitudinal slot cut in its wide wall and two asymmetric impedance vibrators (monopoles) located near the slot outside the waveguide and a monopole located inside the waveguide in the plane $\{x0y\}$ parallel to its narrow wall (Fig. 1). The H_{10}-wave propagates in the waveguide with cross-section $\{a \times b\}$ (the region is marked as Wg) from the direction $z = -\infty$. Parameters of the waveguide filling material are ε_1, μ_1. The slot radiates into half-space marked as Hs located above an infinite perfectly conducting plane. The material parameters of the half-space are ε_2, μ_2. The lengths and radii of the outside monopoles are L_1, L_2 and r_1, r_2, and outer vibrator is displaced relative to the longitudinal slot axis at x_{d1} and x_{d2}. The length and radius of the internal monopole are L_4 and r_4.

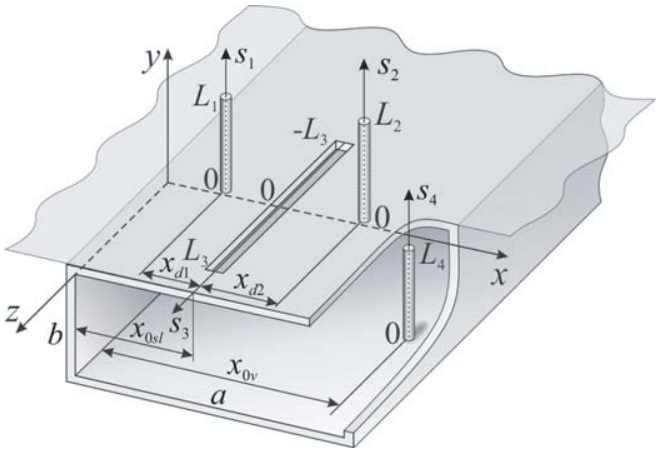

Figure 1. The geometry of the vibrator-slot structure and accepted notations.

Let the slot width and radii of vibrators satisfy the thin radiator approximations: $\frac{r_m}{2L_m} \ll 1$, $\frac{r_m}{\lambda_{1,2}} \ll 1$, $m = 1, 2, 4$, $\frac{d}{2L_3} \ll 1$, $\frac{d}{\lambda_{1,2}} \ll 1$ ($\lambda_{1,2}$ are wavelengths in the corresponding media) and the electric vibrator currents and equivalent magnetic slot current satisfy the boundary conditions $J_m(\pm L_m) = 0$, $J_3(\pm L_3) = 0$ ($-L_m$ are the end coordinates of the monopole mirror images in the plane and waveguide bottom). Then the following system of integral equations can be written [29]

$$
\begin{aligned}
&\left(\frac{\mathrm{d}^2}{\mathrm{d}s_1^2} + k_2^2\right)\left\{\int_{-L_1}^{L_1} J_1\left(s_1'\right) G_{s_1}^{HsE}\left(s_1, s_1'\right) \mathrm{d}s_1' + \int_{-L_2}^{L_2} J_2\left(s_2'\right) G_{s_2}^{HsE}\left(s_1, s_2'\right) \mathrm{d}s_2'\right\} \\
&-ik\vec{e}_{s_1}\mathrm{rot}\int_{-L_3}^{L_3} J_3(s_3') G_{s_3}^{HsM}\left(s_1, s_3'\right) \mathrm{d}s_3' = i\omega\varepsilon_2 z_{i1}(s_1) J_1(s_1), \\
&\left(\frac{\mathrm{d}^2}{\mathrm{d}s_2^2} + k_2^2\right)\left\{\int_{-L_2}^{L_2} J_2\left(s_2'\right) G_{s_2}^{HsE}\left(s_2, s_2'\right) \mathrm{d}s_2' + \int_{-L_1}^{L_1} J_1\left(s_1'\right) G_{s_1}^{HsE}\left(s_2, s_1'\right) \mathrm{d}s_1'\right\} \\
&-ik\vec{e}_{s_2}\mathrm{rot}\int_{-L_3}^{L_3} J_3\left(s_3'\right) G_{s_3}^{HsM}\left(s_2, s_3'\right) \mathrm{d}s_3' = i\omega\varepsilon_2 z_{i2}(s_2) J_2(s_2), \qquad (1) \\
&\frac{1}{\mu_1}\left(\frac{\mathrm{d}^2}{\mathrm{d}s_3^2} + k_1^2\right)\int_{-L_3}^{L_3} J_3\left(s_3'\right) G_{s_3}^{WgM}\left(s_3, s_3'\right) \mathrm{d}s_3' + \frac{1}{\mu_2}\left(\frac{\mathrm{d}^2}{\mathrm{d}s_3^2} + k_2^2\right)\int_{-L_3}^{L_3} J_3\left(s_3'\right) G_{s_3}^{HsM}(s_3, s_3')\mathrm{d}s_3' \\
&+ ik\vec{e}_{s_3}\mathrm{rot}\left\{\begin{array}{l} \displaystyle\int_{-L_1}^{L_1} J_1(s_1') G_{s_1}^{HsE}(s_3, s_1')\mathrm{d}s_1' + \int_{-L_2}^{L_2} J_2(s_2') G_{s_2}^{HsE}(s_3, s_2')\mathrm{d}s_2' \\ \displaystyle + \int_{-L_4}^{L_4} J_4(s_4') G_{s_4}^{WgE}(s_3, s_4')\mathrm{d}s_4' \end{array}\right\} = -i\omega H_{0s_3}(s_3),
\end{aligned}
$$

$$\left(\frac{\mathrm{d}^2}{\mathrm{d}s_4^2}+k_1^2\right)\left\{\int_{-L_4}^{L_4}J_4(s_4')G_{s_4}^{WgE}(s_4,s_4')\mathrm{d}s_4'\right\}$$
$$-ik\vec{e}_{s_4}\mathrm{rot}\int_{-L_3}^{L_3}J_3(s_3')G_{s_3}^{HsM}(s_4,s_3')\mathrm{d}s_3'=-i\omega\varepsilon_1\left[E_{0s_4}(s_4)-z_{i4}(s_4)J_4(s_4)\right],$$

where $z_{im}(s_m)$ are the internal linear impedances of the monopoles ([Ohm/m]); $H_{0s_3}(s_3)$ and $E_{0s_4}(s_4)$ are the projections of the fields of extraneous sources on the slot and monopole axes; $G_{s_{1,2}}^{HsE}(s_{1,2,3},s_{1,2}')$, $G_{s_4}^{WgE}(s_3,s_4')$, and $G_{s_3}^{HsM,WgM(s_{1,2,3,4,s_3'})}$ are the components of the electric (E) and magnetic (M) tensor Green functions for the vector potential of corresponding electrodynamic volumes [1, 3, 4]; $k=2\pi/\lambda$, λ is the wavelength in free space; $k_{1,2}=k\sqrt{\varepsilon_{1,2}\mu_{1,2}}=2\pi/\lambda_{1,2}$, $\vec{e}_{s_m}$, and $\vec{e}_{s_3}$ are unit vectors directed along the vibrator and slot axes; s_m and s_3 are the local coordinates associated with axes of vibrators and slot.

If $\varepsilon_{1,2}=\mu_{1,2}=1$ and $H_{0s_3}(s_3)=H_0\cos\frac{\pi x_{0sl}}{a}e^{-ik_gs_3}=H_0^s(s_3)+H_0^a(s_3)$, $E_{0s_4}(s_4)=H_0\frac{k}{k_g}\sin\frac{\pi x_{0V}}{a}$ (H_0 is the amplitude of the H_{10}-wave), the slot current can be presented as $J_3(s_3)=J_3^s(s_3)+J_3^a(s_3)$. In this expression, $J_3^s(s_3)$ and $J_3^a(s_3)$ are symmetric and antisymmetric components of the slot current relative to the slot center. Hence, Equation (1) can be transformed to:

$$\left(\frac{\mathrm{d}^2}{\mathrm{d}s_1^2}+k^2\right)\left\{\int_{-L_1}^{L_1}J_1(s_1')G_{s_1}^{HsE}(s_1,s_1')\mathrm{d}s_1'+\int_{-L_2}^{L_2}J_2(s_2')G_{s_2}^{HsE}(s_1,s_2')\mathrm{d}s_2'\right\}$$
$$+ik\int_{-L_3}^{L_3}J_3^s(s_3')\tilde{G}_{s_3}^{HsM}(s_1,s_3')\mathrm{d}s_3'=i\omega z_{i1}(s_1)J_1(s_1), \tag{2a}$$
$$\left(\frac{\mathrm{d}^2}{\mathrm{d}s_2^2}+k^2\right)\left\{\int_{-L_2}^{L_2}J_2(s_2')G_{s_2}^{HsE}(s_2,s_2')\mathrm{d}s_2'+\int_{-L_1}^{L_1}J_1(s_1')G_{s_1}^{HsE}(s_2,s_1')\mathrm{d}s_1'\right\}$$
$$+ik\int_{-L_3}^{L_3}J_3^s(s_3')\tilde{G}_{s_3}^{HsM}(s_2,s_3')\mathrm{d}s_3'=i\omega z_{i2}(s_2)J_2(s_2), \tag{2b}$$
$$\left(\frac{\mathrm{d}^2}{\mathrm{d}s_3^2}+k^2\right)\int_{-L_3}^{L_3}J_3^s(s_3')\left[G_{s_3}^{WgM}(s_3,s_3')+G_{s_3}^{HsM}(s_3,s_3')\right]\mathrm{d}s_3'$$
$$-ik\left\{\begin{array}{l}\int_{-L_1}^{L_1}J_1(s_1')\tilde{G}_{s_1}^{HsE}(s_3,s_1')\mathrm{d}s_1'+\int_{-L_2}^{L_2}J_2(s_2')\tilde{G}_{s_2}^{HsE}(s_3,s_2')\mathrm{d}s_2'\\+\int_{-L_4}^{L_4}J_4(s_4')\tilde{G}_{s_4}^{WgE}(s_3,s_4')\mathrm{d}s_4'\end{array}\right\}=-i\omega H_0^s(s_3), \tag{2c}$$
$$\left(\frac{\mathrm{d}^2}{\mathrm{d}s_3^2}+k^2\right)\int_{-L_3}^{L_3}J_3^a(s_3')\left[G_{s_3}^{WgM}(s_3,s_3')+G_{s_3}^{HsM}(s_3,s_3')\right]\mathrm{d}s_3'=-i\omega H_0^a(s_3), \tag{2d}$$
$$\left(\frac{\mathrm{d}^2}{\mathrm{d}s_4^2}+k^2\right)\int_{-L_4}^{L_4}J_4(s_4')G_{s_4}^{WgE}(s_4,s_4')\mathrm{d}s_4'-ik\int_{-L_3}^{L_3}J_3^s(s_3')\tilde{G}_{s_3}^{WgM}(s_4,s_3')\mathrm{d}s_3'$$
$$=-i\omega\left[E_0(s_4)-z_{i4}(s_4)J_4(s_4)\right]. \tag{2e}$$

The solution to the equation system (2) can be found by the generalized method of induced EMMF, using the functions $J_m(s_m)=J_{0m}f_m(s_m)$ and $J_3^{s,a}(s_3)=J_{03}^{s,a}f_3^{s,a}(s_3)$ as approximating expressions for the currents. In the above expressions, J_{0m} and $J_{03}^{s,a}$ are current amplitudes; $f_m(s_m)$ and $f_{03}^{s,a}(s_3)$ are predefined current distribution functions, which can be obtained by solving the equations for currents in a stand-alone vibrator and slot by the averaging method [1, 4]. The following expressions for the distribution function can be obtained:

$$f_1(s_1)=\cos\tilde{k}_1s_1-\cos\tilde{k}_1L_1, \tag{3a}$$
$$f_2(s_2)=\cos\tilde{k}_2s_2-\cos\tilde{k}_2L_2, \tag{3b}$$
$$f_3^s(s_3)=\cos ks_3\cos k_gL_3-\cos kL_3\cos k_gs_3, \tag{3c}$$
$$f_3^a(s_3)=\sin ks_3\sin k_gL_3-\sin kL_3\sin k_gs_3, \tag{3d}$$
$$f_4(s_4)=\cos\tilde{k}_4s_4-\cos\tilde{k}_4L_4, \tag{3e}$$

where $k_g = \frac{2\pi}{\lambda_g} = \sqrt{k^2 - k_c^2}$, $k_c = \frac{2\pi}{\lambda_c} = \frac{\pi}{a}$, λ_g is the wavelength in the waveguide; λ_c is the critical wavelength of H_{10}-wave; $\tilde{k}_m = k + \frac{i\alpha 2\pi z_{im}^{av}}{Z_0}$, $z_{im}^{av} = \frac{1}{2L_m}\int_{-L_m}^{L_m} z_{im}(s_m)\mathrm{d}s_m$ are the impedances averaged over the vibrator length, and $Z_0 = 120\pi$ Ohm.

Let us first multiply each of Equations (2a), (2b), (2c), and (2d) by functions $f_1(s_1)$, $f_2(s_2)$, $f_3^s(s_3)$, $f_3^a(s_3)$, and $f_4(s_4)$, respectively, and then integrate the multiplication results over the vibrator and slot length lengths. Thus, the following system of linear algebraic equations (SLAE) can be obtained

$$\begin{cases} J_{01}\left(Z_{11} + F_1^{\bar{Z}}\right) + J_{02}Z_{12} + J_{03}^s Z_{13} = 0, \\ J_{02}\left(Z_{22} + F_2^{\bar{Z}}\right) + J_{01}Z_{21} + J_{03}^s Z_{23} = 0, \\ J_{03}^s\left(Z_{33}^{sWg} + Z_{33}^{sHs}\right) + J_{01}Z_{31} + J_{02}Z_{32} + J_{04}Z_{34} = -\dfrac{i\omega}{2k}H_3^s, \\ J_{03}^a\left(Z_{33}^{aWg} + Z_{33}^{aHs}\right) = -\dfrac{i\omega}{2k}H_3^a, \\ J_{04}\left(Z_{44} + F_4^{\bar{Z}}\right) + J_{03}^s Z_{43} = -\dfrac{i\omega}{2k}E_4, \end{cases} \tag{4}$$

where $H_3^s = H_0\cos\frac{\pi x_{0sl}}{a}\int_{-L_3}^{L_3}\cos k_g s_3 f_3^s(s_3)\mathrm{d}s_3$, $H_3^a = -iH_0\cos\frac{\pi x_{0sl}}{a}\int_{-L_3}^{L_3}\sin k_g s_3 f_3^a(s_3)\mathrm{d}s_3$, $E_4 = H_0\frac{k}{k_g}\sin\frac{\pi x_{0V}}{a}\int_{-L_4}^{L_4} f_4(s_4)\mathrm{d}s_4$, Z_{mn} $(m,n = 1,2,3,4)$ and $F_m^{\bar{Z}}$ are dimensionless coefficients. When the amplitudes of currents J_{0m} and $J_{03}^{s,a}$ are found as the solution of system in Eq. (4), the electrodynamic characteristics of this vibrator-slot structure can be easily obtained.

3. GENERAL ANALYSIS OF THE CLAVIN ELEMENT

The following relations for the Clavin element are valid: $2L_1 = 2L_2 = 2L_v$, $r_1 = r_2 = r$, $\alpha_1 = \alpha_2 = \alpha$, $2L_4 = 2L_V$, $r_4 = r_V$, $\alpha_4 = \alpha_V$, $\bar{Z}_{S1}(s_1) = \bar{Z}_{S2}(s_2) = \bar{Z}_S(s_v) = 2\pi r_v z_{iv}(s_v)/Z_0$, $\bar{Z}_{S4}(s_4) = \bar{Z}_{SV}(s_V) = 2\pi r_V z_{iV}(s_V)/Z_0$, $\tilde{k}_1 = \tilde{k}_2 = \tilde{k} = k + i(\alpha/r)\bar{Z}_S^{av}$, $\tilde{k}_4 = \tilde{k}_V = k + i(\alpha_V/r_V)\bar{Z}_{SV}^{av}$, $x_{d1} = x_{d2} = x_d$, $F_1^{\bar{Z}} = F_2^{\bar{Z}} = F_v^{\bar{Z}}$, $F_4^{\bar{Z}} = F_V^{\bar{Z}}$, $H_3^{s,a} = H_{sl}^{s,a}$, $(Z_{33}^{s,aWg} + Z_{33}^{s,aHs}) = Z_{sl}^{s,a\Sigma}$, $f_1(s_1) = f_2(s_2) = f_v(s_v)$, $f_4(s_4) = f_V(s_V)$, $f_3^{s,a}(s_3) = f_{sl}^{s,a}(s_{sl})$, $Z_{11} + F_1^{\bar{Z}} = Z_{22} + F_2^{\bar{Z}} = Z_v + F_v^{\bar{Z}} = Z_v^{\Sigma}$, $Z_{44} + F_4^{\bar{Z}} = Z_V^{\Sigma}$, $Z_{12} = Z_{21} = Z_{vv}$, $Z_{13} = Z_{23} = -2Z_{31} = -2Z_{32} = Z_c$, $Z_{34} = -Z_{43} = Z_{Wg}$.

Therefore, the SLAE (4) can be transformed as follows:

$$\begin{cases} J_{0v}Z_v^{\Sigma} + J_{0v}Z_{vv} + J_{0sl}^s Z_c = 0, \\ J_{0sl}^s Z_{sl}^{s\Sigma} - J_{0v}Z_c + J_{0V}Z_{Wg} = -\dfrac{i\omega}{2k}H_{sl}^s, \\ J_{0sl}^a Z_{sl}^{a\Sigma} = -\dfrac{i\omega}{2k}H_{sl}^a, \\ J_{0V}Z_V^{\Sigma} - J_{0sl}^s Z_{Wg} = -\frac{i\omega}{2k}E_V. \end{cases} \tag{5}$$

The solution of equations system (5) can be written as:

$$\begin{aligned} J_{0v} &= \frac{i\omega}{2k}HE\frac{Z_c}{\tilde{Z}_{sl}\tilde{Z}_v + Z_c^2}, \quad J_{0V} = -\frac{i\omega}{2k}\left[E_V\frac{1}{Z_V^{\Sigma}} + HE\frac{\tilde{Z}_v Z_{Wg}}{(\tilde{Z}_{sl}\tilde{Z}_v + Z_c^2)Z_V^{\Sigma}}\right], \\ J_{0sl}^s &= -\frac{i\omega}{2k}HE\frac{\tilde{Z}_v}{\tilde{Z}_{sl}\tilde{Z}_v + Z_c^2}, \quad J_{0sl}^a = -\frac{i\omega}{2k}H_{sl}^a\frac{1}{Z_{sl}^{a\Sigma}}. \end{aligned} \tag{6}$$

where $\tilde{Z}_v = Z_v^{\Sigma} + Z_{vv}$, $\tilde{Z}_{sl} = Z_{sl}^{s\Sigma} + Z_{Wg}^2/Z_V^{\Sigma}$, $HE = H_{sl}^s - E_V Z_{Wg}/Z_V^{\Sigma}$. The components of the tensor Green functions for the Clavin element can be written as:

$$G_{s_{v(vv)}}^{HsE}\left(s_v, s_v'\right) = \frac{e^{-ik\sqrt{(s_v - s_v')^2 + r^2(4x_d^2)}}}{\sqrt{(s_v - s_v')^2 + r^2(4x_d^2)}}, \quad G_{s_{sl}}^{HsM}\left(s_{sl}, s_{sl}'\right) = 2\frac{e^{-ik\sqrt{\left(s_{sl} - s_{sl}'\right)^2 + (d_e/4)^2}}}{\sqrt{\left(s_{sl} - s_{sl}'\right)^2 + (d_e/4)^2}},$$

$$
\begin{aligned}
G_{s_{sl}}^{WgM}\left(s_{sl},s'_{sl}\right) &= \frac{2\pi}{ab}\sum_{m=0}^{\infty}\sum_{n=0}^{\infty}\frac{\varepsilon_m\varepsilon_n}{k_z}e^{-k_z|s_{sl}-s'_{sl}|}\cos k_x x_0\cos k_x\left(x_0+\frac{d_e}{4}\right),\\
\tilde{G}_{s_v}^{HsE}\left(s_{sl},s'_v\right) &= \frac{\partial}{\partial x_{Hs}}G_{s_v}^{HsE}\left[x_{Hs},0,z_{Hs}(s_{sl});x_d,y'_{Hs}\left(s'_v\right),0\right]\quad\text{at}\quad x_{Hs}=0,\\
\tilde{G}_{s_{sl}}^{HsM}(s_v,s'_{sl}) &= \frac{\partial}{\partial x_{Hs}}G_{s_{sl}}^{HsM}\left[x_{Hs},y_{Hs}(s_v),0;0,0,z'_{Hs}\left(s'_{sl}\right)\right]\quad\text{at}\quad x_{Hs}=x_d,\\
\tilde{G}_{s_V}^{WgE}\left(s_{sl},s'_V\right) &= \frac{\partial}{\partial x_{Wg}}G_{s_V}^{WgE}\left[x_{Wg},0,z_{Wg}(s_{sl});\cos k_x x_{0V},y_{Wg}\left(s'_V\right),0\right]\quad\text{at}\quad x_{Wg}=x_{0sl},\\
\tilde{G}_{s_{sl}}^{WgM}\left(s_V,s'_{sl}\right) &= \frac{\partial}{\partial x_{Wg}}G_{s_{sl}}^{WgM}\left[x_{Wg},y_{Wg}(s_V),0;\cos k_x x_{0sl},0,z'_{Wg}\left(s'_{sl}\right)\right]\quad\text{at}\quad x_{Wg}=x_{0V}.
\end{aligned}
$$

where $\varepsilon_n=\begin{cases}1, & n=0\\ 2, & n\neq 0\end{cases}$, $k_x=\frac{m\pi}{a}$, $k_y=\frac{n\pi}{b}$, $k_z=\sqrt{k_x^2+k_y^2-k^2}$, m and n are integers; $d_e\approx d\exp(-\frac{\pi h}{2d})$ is the effective slot width [1], which takes into account the thickness h of the waveguide wall. All quantities in the expressions for the current amplitudes in Eq. (6) are:

$$
\begin{aligned}
Z_{v(vv)} &= \frac{1}{2k}\int_{-L_v}^{L_v}f_v(s)\left[\int_{-L_v}^{L_v}f_v(s')\left(\frac{\mathrm{d}^2}{\mathrm{d}s^2}+k^2\right)G_{s_{v(vv)}}^{HsE}(s,s')\mathrm{d}s'\right]\mathrm{d}s\\
&= \left(\frac{\tilde{k}}{k}\right)\sin\tilde{k}L_vF_{v(vv)}(L_v)-\frac{k}{2}\cos\tilde{k}L_v\int_{-L_v}^{L_v}F_{v(vv)}(s)\mathrm{d}s+\frac{k^2-\tilde{k}^2}{2k}\int_{-L_v}^{L_v}\cos\tilde{k}sF_{v(vv)}(s)\mathrm{d}s,\\
F_{v(vv)}(s) &= \int_{-L_v}^{L_v}f_v(s')\frac{e^{-ik\sqrt{(s-s')^2+r^2(4x_d^2)}}}{\sqrt{(s-s')^2+r^2(4x_d^2)}}\mathrm{d}s',\\
F_v^{\bar{Z}} &= -\frac{i}{r}\int_0^{L_v}f_v^2(s)\bar{Z}_S(s)\mathrm{d}s,F_V^{\bar{Z}}=-\frac{i}{r_V}\int_0^{L_V}f_V^2(s)\bar{Z}_{SV}(s)\mathrm{d}s,
\end{aligned}
\tag{7}
$$

where $\bar{Z}_S(s)=\bar{R}_S+i\bar{X}_S\phi(s)$, $\bar{Z}_{SV}(s)=\bar{R}_{SV}+i\bar{X}_{SV}\phi_V(s)$, $\phi(s)$ and $\phi_V(s)$ are predefined functions,

$$
\begin{aligned}
Z_c &= ix_d\int_{-L_v}^{L_v}f(s)\left\{\int_{-L_{sl}}^{L_{sl}}f_{sl}^s(s')\left[\frac{e^{-ik\sqrt{s^2+s'^2+x_d^2}}}{(s^2+s'^2+x_d^2)^{3/2}}\left(ik\sqrt{s^2+s'^2+x_d^2}+1\right)\right]\mathrm{d}s'\right\}\mathrm{d}s,\\
Z_{sl}^{s(a)Hs\{Wg\}} &= \frac{1}{2k}\int_{-L_{sl}}^{L_{sl}}f_{sl}^{s(a)}(s)\left[\int_{-L_{sl}}^{L_{sl}}f_{sl}^{s(a)}(s')\left(\frac{\mathrm{d}^2}{\mathrm{d}s^2}+k^2\right)G_{s_{sl}}^{Hs\{Wg\}M}(s,s')\mathrm{d}s'\right]\mathrm{d}s,\\
Z_{sl}^{sHs} &= 2\left\{\begin{array}{l}\left[\left(\frac{k_g}{k}\right)\cos kL_{sl}\sin k_gL_{sl}-\sin kL_{sl}\cos k_gL_{sl}\right]F_{sl}^s(L_{sl})\\ +k\cos k_gL_{sl}\int_{-L_{sl}}^{L_{sl}}\cos ksF_{sl}^s(s)\mathrm{d}s-\frac{k^2+k_g^2}{2k}\cos kL_{sl}\int_{-L_{sl}}^{L_{sl}}\cos k_gsF_{sl}^s(s)\mathrm{d}s\end{array}\right\},\\
Z_{sl}^{aHs} &= 2\left\{\begin{array}{l}\left[\left(\frac{k_g}{k}\right)\sin kL_{sl}\cos k_gL_{sl}-\cos kL_{sl}\sin k_gL_{sl}\right]F_{sl}^a(L_{sl})\\ +k\sin k_gL_{sl}\int_{-L_{sl}}^{L_{sl}}\sin ksF_{sl}^a(s)\mathrm{d}s-\frac{k^2-k_g^2}{2k}\sin kL_{sl}\int_{-L_{sl}}^{L_{sl}}\sin k_gsF_{sl}^a(s)\mathrm{d}s\end{array}\right\},\\
F_{sl}^{s(a)}(s) &= \int_{-L_{sl}}^{L_{sl}}f_{sl}^{s(a)}(s')\frac{e^{-ik\sqrt{(s-s')^2+(d_e/4)^2}}}{\sqrt{(s-s')^2+(d_e/4)^2}}\mathrm{d}s',\\
Z_{sl}^{sWg} &= \frac{2\pi}{ab}\sum_{m=0}^{\infty}\sum_{n=0}^{\infty}\frac{\varepsilon_m\varepsilon_n}{k^2}\cos k_xx_0\cos k_x\left(x_0+\frac{d_e}{4}\right)
\end{aligned}
$$

$$\times\left\{\begin{array}{l}\left[\cos k_gL_{sl}\left(\dfrac{k}{k_z}\sin kL_{sl}-\cos kL_{sl}\right)\right]F_e^s\\ -\dfrac{\cos kL_{sl}}{k_z^2+k_g^2}\left[(k_z^2+k^2)\left(\dfrac{k_g}{k_z}\sin k_gL_{sl}-\cos k_gL_{sl}\right)F_e^s+k_c^2F_k^s\right]\end{array}\right\},$$

$$F_e^s = \frac{k\cos k_gL_{sl}}{k_z^2+k^2}\left[k_z\cos kL_{sl}\left(1-e^{-2k_zL_{sl}}\right)+k\sin kL_{sl}\left(1+e^{-2k_zL_{sl}}\right)\right]$$
$$-\frac{k\cos kL_{sl}}{k_z^2+k_g^2}\left[k_z\cos k_gL_{sl}\left(1-e^{-2k_zL_{sl}}\right)+k_g\sin k_gL_{sl}\left(1+e^{-2k_zL_{sl}}\right)\right],$$

$$F_k^s = 2\cos k_gL_{sl}\frac{\sin kL_{sl}\cos k_gL_{sl}-(k_g/k)\cos kL_{sl}\sin k_gL_{sl}}{1-(k_g/k)^2}-\cos kL_{sl}\frac{\sin 2k_gL_{sl}+2k_gL_{sl}}{2(k_g/k)},$$

$$Z_{sl}^{aWg} = \frac{2\pi}{ab}\sum_{m=0}^{\infty}\sum_{n=0}^{\infty}\frac{\varepsilon_m\varepsilon_n}{k^2}\cos k_xx_0\cos k_x\left(x_0+\frac{d_e}{4}\right)$$
$$\times\left\{\begin{array}{l}\left[-\sin k_gL_{sl}\left(\dfrac{k}{k_z}\cos kL_{sl}+\sin kL_{sl}\right)\right]F_e^a\\ +\dfrac{\sin kL_{sl}}{k_z^2+k_g^2}\left[(k_z^2+k^2)\left(\dfrac{k_g}{k_z}\cos k_gL_{sl}+\sin k_gL_{sl}\right)F_e^a+k_c^2F_k^a\right]\end{array}\right\},$$

$$F_e^a = \frac{k\sin k_gL_{sl}}{k_z^2+k^2}\left[k_z\sin kL_{sl}\left(1+e^{-2k_zL_{sl}}\right)-k\cos kL_{sl}\left(1-e^{-2k_zL_{sl}}\right)\right]$$
$$-\frac{k\sin kL_{sl}}{k_z^2+k_g^2}\left[k_z\sin k_gL_{sl}\left(1+e^{-2k_zL_{sl}}\right)-k_g\cos k_gL_{sl}\left(1-e^{-2k_zL_{sl}}\right)\right],$$

$$F_k^a = 2\sin k_gL_{sl}\frac{\cos kL_{sl}\sin k_gL_{sl}-(k_g/k)\sin kL_{sl}\cos k_gL_{sl}}{1-(k_g/k)^2}-\sin kL_{sl}\frac{\sin 2k_gL_{sl}-2k_gL_{sl}}{2(k_g/k)},$$

$$Z_V = \frac{4\pi}{ab}\sum_{m=1}^{\infty}\sum_{n=0}^{\infty}\frac{\varepsilon_n\left(k^2-k_y^2\right)\tilde{k}_V^2}{kk_z\left(\tilde{k}_V^2-k_y^2\right)^2}e^{-k_zr_V}\sin^2k_xx_{0V}\left[\sin\tilde{k}_VL_V\cos k_yL_V-\left(\tilde{k}_V/k_y\right)\cos\tilde{k}L_V\sin k_yL_V\right]^2,$$

$$Z_{Wg} = \frac{4\pi}{ab}\sum_{m=1}^{\infty}\sum_{n=0}^{\infty}\frac{\varepsilon_nk_x\tilde{k}_V}{kk_z\left(\tilde{k}_V^2-k_y^2\right)}e^{k_zL_{sl}}\sin k_xx_{0V}\cos k_xx_{0sl}$$
$$\times F_e^s\left[\sin\tilde{k}_VL_V\cos k_yL_V-\left(\tilde{k}_V/k_y\right)\cos\tilde{k}L_V\sin k_yL_V\right],$$

$$H_{sl}^{s(a)} = \frac{1(-i)}{k}H_0\cos\frac{\pi x_{0sl}}{a}F_k^{s(a)},$$

$$E_V = H_0\frac{k}{k_g\tilde{k}_V}\sin\frac{\pi x_{0V}}{a}f\left(\tilde{k}_VL_V\right),F_V=\sin\tilde{k}_VL_V-\tilde{k}_VL_V\cos\tilde{k}_VL_V.$$

Then, the final expressions for the currents based on Eq. (3) can be written as:

$$\begin{aligned}J_v(s_v) &= -\frac{i\omega}{2k^2}H_0J_vf_v(s_v),\quad J_V(s_V)=-\frac{i\omega}{2k^2}H_0J_Vf_V(s_V),\\ J_{sl}(s_{sl}) &= -\frac{i\omega}{2k^2}H_0\left[J_{sl}^sf_{sl}^s(s_{sl})+iJ_{sl}^af_{sl}^a(s_{sl})\right],\end{aligned}\tag{8}$$

where

$$J_v = -\frac{Z_cF_{sl,V}}{\tilde{Z}_{sl}\tilde{Z}_v+Z_c^2},\quad J_V=\frac{k^2\sin(\pi x_{0V}/a)F_V}{k_g\tilde{k}_VZ_V^{\Sigma}}+\frac{\tilde{Z}_vZ_{Wg}F_{sl,V}}{(\tilde{Z}_{sl}\tilde{Z}_v+Z_c^2)Z_V^{\Sigma}},$$
$$J_{sl}^s = \frac{\tilde{Z}_vF_{sl,V}}{\tilde{Z}_{sl}\tilde{Z}_v+Z_c^2},\quad J_{sl}^a=-\cos\frac{\pi x_{0sl}}{a}\frac{F_k^a}{Z_{sl}^{a\Sigma}},\quad F_{sl,V}=\cos\frac{\pi x_{0sl}}{a}F_k^s-\frac{k^2}{k_g\tilde{k}_V}\sin\frac{\pi x_{0V}}{a}F_V.$$

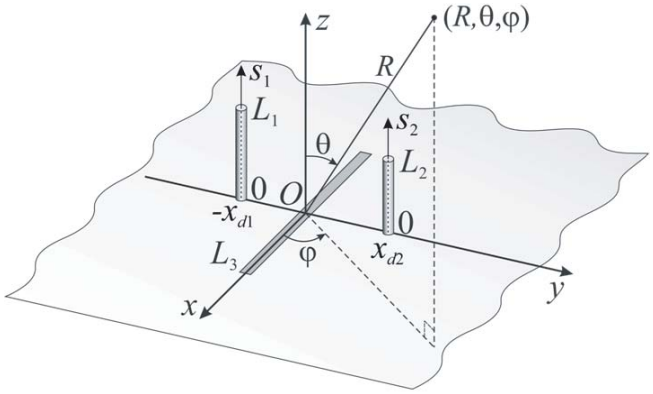

Figure 2. Coordinate system for determining the electric field of the vibrator-slot structure.

These expressions allow us to define the electrodynamic characteristics of the Clavin element. The field reflection and transmission coefficients, S_{11} and S_{12}, in the waveguide and the power radiation coefficient $|S_\Sigma|^2$ can be written in the form:

$$S_{11} = -\frac{2\pi}{iabk_g k}\left[\frac{k_c^2}{k^2}\cos\frac{\pi x_{0sl}}{a}\left(J_{sl}^s F_k^s + J_{sl}^a F_k^a\right) - \frac{2k_g}{\tilde{k}_V}\sin\frac{\pi x_{0V}}{a} J_V F_V\right] e^{2ik_g z}, \tag{9}$$

$$S_{12} = 1 - \frac{2\pi}{iabk_g k}\left[\frac{k_c^2}{k^2}\cos\frac{\pi x_{0sl}}{a}\left(J_{sl}^s F_k^s - J_{sl}^a F_k^a\right) + \frac{2k_g}{\tilde{k}_V}\sin\frac{\pi x_{0V}}{a} J_V F_V\right], \tag{10}$$

$$|S_\Sigma|^2 = 1 - |S_{11}|^2 - |S_{12}|^2. \tag{11}$$

Formulas (8)–(11) are obtained by assuming that $H_0 = 1$, and the vibrators are losses. In the spherical coordinate system shown in Fig. 2, the far-zone electric field of the Clavin element is defined by the expression

$$\vec{E}(R,\theta,\varphi) = \frac{ik^2}{\omega}\frac{e^{-ikR}}{R}\left[\vec{\theta}^0 \sin\theta\left(\tilde{E}_1 e^{-ikx_{d1}\sin\theta\sin\varphi} + \tilde{E}_2 e^{ikx_{d2}\sin\theta\sin\varphi}\right) + \left(\vec{\varphi}^0\cos\theta\cos\varphi + \vec{\theta}^0\sin\varphi\right)2\tilde{E}_3\right], \tag{12}$$

where $\vec{\theta}^0$ and $\vec{\varphi}^0$ are unit vectors, $\tilde{E}_1 = J_{01}f_{C1}$, $\tilde{E}_2 = J_{02}f_{C2}$, $\tilde{E}_3 = J_{03}^s f_{C3}^s + J_{03}^a f_{C3}^a$;

$$f_{C1} = \int_{-L_1}^{L_1} f_1(z)e^{ikz\cos\theta}\mathrm{d}z, \quad f_{C2} = \int_{-L_2}^{L_2} f_2(z)e^{ikz\cos\theta}\mathrm{d}z, \quad f_{C3}^{s(a)} = \int_{-L_3}^{L_3} f_3^{s(a)}(x)e^{ikx\sin\theta\cos\varphi}\mathrm{d}x.$$

Then, in accordance with formulas (3), we obtain:

$$\begin{aligned}
f_{Cm} &= \frac{2}{\tilde{k}_m^2 - (k\cos\theta)^2}\left[\tilde{k}_m\cos\left(kL_m\cos\theta\right)\sin\left(\tilde{k}_m L_m\right) - k\sin\left(kL_m\cos\theta\right)\cos\left(\tilde{k}_m L_m\right)\cos\theta\right] \\
&\quad -2L_m\cos\left(\tilde{k}_m L_m\right)\frac{\sin\left(kL_m\cos\theta\right)}{kL_m\cos\theta}, \quad m = 1,2; \\
f_{C3}^s &= \frac{2\cos(k_g L_3)}{k - k(\sin\theta\cos\varphi)^2}\left[\cos(kL_3\sin\theta\cos\varphi)\sin(kL_3) - \sin(kL_3\sin\theta\cos\varphi)\cos(kL_3)\sin\theta\cos\varphi\right] \\
&\quad -\frac{2\cos(kL_3)}{k_g^2 - (k\sin\theta\cos\varphi)^2}\left[k_g\cos(kL_3\sin\theta\cos\varphi)\sin(k_g L_3)\right. \\
&\quad \left.-k\sin(kL_3\sin\theta\cos\varphi)\cos(k_g L_3)\sin\theta\cos\varphi\right], \\
f_{C3}^a &= \frac{2i\sin(k_g L_3)}{k - k(\sin\theta\cos\varphi)^2}\left[-\sin(kL_3\sin\theta\cos\varphi)\cos(kL_3) + \cos(kL_3\sin\theta\cos\varphi)\sin(kL_3)\sin\theta\cos\varphi\right] \\
&\quad -\frac{2i\sin(kL_3)}{k_g^2 - (k\sin\theta\cos\varphi)^2}\left[-k_g\sin(kL_3\sin\theta\cos\varphi)\cos(k_g L_3)\right. \\
&\quad \left.+k\cos(kL_3\sin\theta\cos\varphi)\sin(k_g L_3)\sin\theta\cos\varphi\right].
\end{aligned}$$

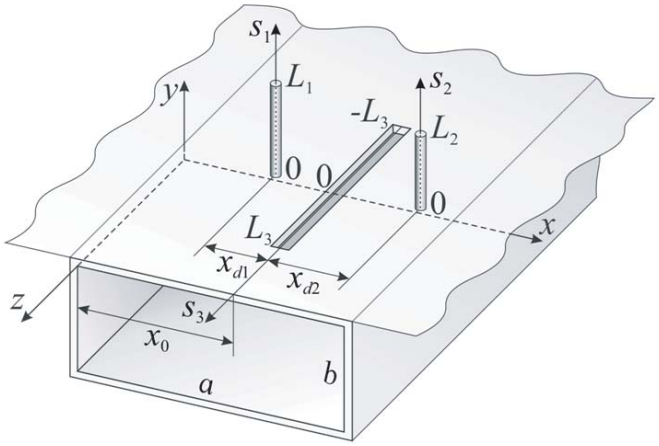

Figure 3. The geometry of the problem and accepted notations.

4. VIBRATOR-SLOT RADIATOR BASED ON A HOLLOW RECTANGULAR WAVEGUIDE

If the combined radiator does not include the internal vibrator (Fig. 3), the SLAE (4) can be simplified to

$$\begin{cases} J_{01}Z_{11}^{\Sigma} + J_{02}Z_{12} + J_{03}^{s}Z_{13} = 0, \\ J_{02}Z_{11}^{\Sigma} + J_{01}Z_{21} + J_{03}^{s}Z_{23} = 0, \\ J_{03}^{s}Z_{33}^{s\Sigma} + J_{01}Z_{31} + J_{02}Z_{32} = -\dfrac{i\omega}{2k}H_3^s, \\ J_{03}^{a}Z_{33}^{a\Sigma} = -\dfrac{i\omega}{2k}H_3^a, \end{cases} \tag{13}$$

where $Z_{11}^{\Sigma} = Z_{11} + F_1^{\bar{Z}}$, $Z_{22}^{\Sigma} = Z_{22} + F_2^{\bar{Z}}$, $Z_{33}^{s(a)\Sigma} = Z_{33}^{s(a)Wg} + Z_{33}^{s(a)Hs}$.

Solution of equations system (13) can be written as

$$J_{01} = \frac{i\omega}{2k}H_3^s\frac{Z_{22}^{\Sigma}Z_{13} - Z_{23}Z_{12}}{Z_{33}^{s\Sigma}\tilde{Z}_{12} + Z_{31}\tilde{Z}_{22} + Z_{32}\tilde{Z}_{11}}, \quad J_{02} = \frac{i\omega}{2k}H_3^s\frac{Z_{11}^{\Sigma}Z_{23} - Z_{13}Z_{21}}{Z_{33}^{s\Sigma}\tilde{Z}_{12} + Z_{31}\tilde{Z}_{22} + Z_{32}\tilde{Z}_{11}}, \tag{14a}$$

$$J_{03}^{s} = -\frac{i\omega}{2k}H_3^s\frac{\tilde{Z}_{12}}{Z_{33}^{s\Sigma}\tilde{Z}_{12} + Z_{31}\tilde{Z}_{22} + Z_{32}\tilde{Z}_{11}}, \quad J_{03}^{a} = -\frac{i\omega}{2k}H_3^s\frac{1}{Z_{33}^{a\Sigma}}. \tag{14b}$$

Since $H_3^{s(a)} = \frac{1(-i)}{k}H_0\cos\frac{\pi x_0}{a}F_k^{s(a)}$, the final expressions for the currents can be presented as:

$$J_1(s_1) = \frac{i\omega}{2k^2}H_0J_1f_1(s_1), \quad J_2(s_2) = \frac{i\omega}{2k^2}H_0J_2f_2(s_2), \tag{15a}$$

$$J_3(s_3) = -\frac{i\omega}{2k^2}H_0\left[J_3^sf_3^s(s_3) + iJ_3^af_3^a(s_3)\right], \tag{15b}$$

where

$$J_1 = \cos\frac{\pi x_0}{a}F_k^s\frac{Z_{22}^{\Sigma}Z_{13} - Z_{23}Z_{12}}{Z_{33}^{s\Sigma}\tilde{Z}_{12} + Z_{31}\tilde{Z}_{22} + Z_{32}\tilde{Z}_{11}}, \quad J_2 = \cos\frac{\pi x_0}{a}F_k^s\frac{Z_{11}^{\Sigma}Z_{23} - Z_{13}Z_{21}}{Z_{33}^{s\Sigma}\tilde{Z}_{12} + Z_{31}\tilde{Z}_{22} + Z_{32}\tilde{Z}_{11}}, \tag{16a}$$

$$J_3^s = \cos\frac{\pi x_0}{a}F_k^s\frac{\tilde{Z}_{12}}{Z_{33}^{s\Sigma}\tilde{Z}_{12} + Z_{31}\tilde{Z}_{22} + Z_{32}\tilde{Z}_{11}}, \quad J_3^a = -\cos\frac{\pi x_0}{a}F_k^a\frac{1}{Z_{33}^{a\Sigma}}, \tag{16b}$$

$$\tilde{Z}_{12} = Z_{11}^{\Sigma}Z_{22}^{\Sigma} - Z_{12}Z_{21}, \quad \tilde{Z}_{11} = Z_{13}Z_{21} - Z_{11}^{\Sigma}Z_{23}, \quad \tilde{Z}_{22} = Z_{23}Z_{12} - Z_{22}^{\Sigma}Z_{13}.$$

After substitution the amplitude $H_0 = 1$ in formulas (15a) and (15b), the radiation field is determined

by formula (12). The energy characteristics of this structure can be obtained in the form:

$$S_{11} = -\frac{2\pi k_c^2}{iabk_g k^3}\cos\frac{\pi x_0}{a}\left(J_3^s F_k^s + J_3^a F_k^a\right)e^{2ik_g z}, \tag{17}$$

$$S_{12} = 1 - \frac{2\pi k_c^2}{iabk_g k^3}\cos\frac{\pi x_0}{a}\left(J_3^s F_k^s - J_3^a F_k^a\right), \tag{18}$$

$$|S_\Sigma|^2 = 1 - |S_{11}|^2 - |S_{12}|^2, \tag{19}$$

The components of the Green functions for this case can be written in the form:

$$G_{s_{1(2)}}^{HsE}\left(s_{1(2)}, s'_{1(2)}\right) = \frac{e^{-ik\sqrt{\left(s_{1(2)}-s'_{1(2)}\right)^2+r_{1(2)}^2}}}{\sqrt{\left(s_{1(2)}-s'_{1(2)}\right)^2+r_{1(2)}^2}},$$

$$G_{s_{1(2)}}^{HsE}\left(s_{1(2)}, s'_{2(1)}\right) = \frac{e^{-ik\sqrt{\left(s_{1(2)}-s'_{2(1)}\right)^2+\left(x_{d1}+x_{d2}\right)^2}}}{\sqrt{\left(s_{1(2)}-s'_{2(1)}\right)^2+\left(x_{d1}+x_{d2}\right)^2}},$$

$$G_{s_3}^{HsM}\left(s_3, s'_3\right) = 2\frac{e^{-ik\sqrt{\left(s_3-s'_3\right)^2+\left(d_e/4\right)^2}}}{\sqrt{\left(s_3-s'_3\right)^2+\left(d_e/4\right)^2}},$$

$$\tilde{G}_{s_{1(2)}}^{HsE}\left(s_3, s'_{1(2)}\right) = \frac{\partial}{\partial x_{Hs}}G_{s_{1(2)}}^{HsE}\left[x_{Hs}, 0, z_{Hs}(s_3); x_{d1(2)}, y'_{Hs}\left(s'_{1(2)}\right), 0\right] \quad \text{at} \quad x_{Hs}=0,$$

$$\tilde{G}_{s_3}^{HsM}\left(s_{1(2)}, s'_3\right) = \frac{\partial}{\partial x_{Hs}}G_{s_3}^{HsM}\left[x_{Hs}, y_{Hs}\left(s_{1(2)}\right), 0; 0, 0, z'_{Hs}\left(s'_3\right)\right] \quad \text{at} \quad x_{Hs}=x_{d1(2)}.$$

Then, the corresponding coefficients in formulas (14) and (16) are:

$$\begin{aligned}
Z_{11(22)} &= \frac{1}{2k}\int_{-L_{1(2)}}^{L_{1(2)}} f_{1(2)}\left(s_{1(2)}\right)\left[\int_{-L_{1(2)}}^{L_{1(2)}} f_{1(2)}\left(s'_{1(2)}\right)\left(\frac{\mathrm{d}^2}{\mathrm{d}s_{1(2)}^2}+k^2\right)G_{s_{1(2)}}^{HsE}\left(s_{1(2)}, s'_{1(2)}\right)\mathrm{d}s'_{1(2)}\right]\mathrm{d}s_{1(2)} \\
&= \left(\frac{\tilde{k}_{1(2)}}{k}\right)\sin\tilde{k}_{1(2)}L_{1(2)}F_{1(2)}(L_{1(2)}) - \frac{k}{2}\cos\tilde{k}_{1(2)}L_{1(2)}\int_{-L_{1(2)}}^{L_{1(2)}} F_{1(2)}(s_{1(2)})\mathrm{d}s_{1(2)} \\
&+ \frac{k^2-\tilde{k}_{1(2)}^2}{2k}\int_{-L_{1(2)}}^{L_{1(2)}}\cos\tilde{k}_{1(2)}s_{1(2)}F_{1(2)}(s_{1(2)})\mathrm{d}s_{1(2)},
\end{aligned}$$

$$F_{1(2)}(s_{1(2)}) = \int_{-L_{1(2)}}^{L_{1(2)}} f_{1(2)}\left(s'_{1(2)}\right)\frac{e^{-ik\sqrt{\left(s_{1(2)}-s'_{1(2)}\right)^2+r_{1(2)}^2}}}{\sqrt{\left(s_{1(2)}-s'_{1(2)}\right)^2+r_{1(2)}^2}}\mathrm{d}s'_{1(2)}, \tag{20}$$

$$\begin{aligned}
Z_{12} = Z_{21} &= \frac{1}{2k}\int_{-L_1}^{L_1} f_1(s_1)\left[\int_{-L_2}^{L_2} f_2\left(s'_2\right)\left(\frac{\mathrm{d}^2}{\mathrm{d}s_1^2}+k^2\right)G_{s_2}^{HsE}\left(s_1, s'_2\right)\mathrm{d}s'_2\right]\mathrm{d}s_1 \\
&= \left(\frac{\tilde{k}_1}{k}\right)\sin\tilde{k}_1L_1F_{12}(L_1) - \frac{k}{2}\cos\tilde{k}_1L_1\int_{-L_1}^{L_1}F_{12}(s_1)\mathrm{d}s_1 + \frac{k^2-\tilde{k}_1^2}{2k}\int_{-L_1}^{L_1}\cos\tilde{k}_1s_1F_{12}(s_1)\mathrm{d}s_1,
\end{aligned}$$

$$F_{12}(s_{12}) = \int_{-L_2}^{L_2} f_2\left(s'_2\right)\frac{e^{-ik\sqrt{\left(s_1-s'_2\right)^2+\left(x_{d1}+x_{d2}\right)^2}}}{\sqrt{\left(s_1-s'_2\right)^2+\left(x_{d1}+x_{d2}\right)^2}}\mathrm{d}s'_2,$$

$$F_{1(2)}^{\bar{Z}} = -\frac{i}{r_{1(2)}}\int_0^{L_{1(2)}} f_{1(2)}^2(s_{1(2)})\bar{Z}_{S1(2)}\left(s_{1(2)}\right)\mathrm{d}s_{1(2)},$$

where $\bar{Z}_{S1(2)}(s_{1(2)}) = \bar{R}_{S1(2)} + i\bar{X}_{S1(2)}\phi_{1(2)}(s_{1(2)})$, $\phi_{1(2)}(s_{1(2)})$ are predefined functions,

$$Z_{1(2)3} = 2ix_{d1(2)} \int_{-L_{1(2)}}^{L_{1(2)}} f_{1(2)}\left(s_{1(2)}\right) \left\{ \int_{-L_3}^{L_3} f_3^s\left(s'_3\right) \left[\frac{e^{-ik\sqrt{s_{1(2)}^2+s_3'^2+x_{d1(2)}^2}}}{\left(s_{1(2)}^2+s_3'^2+x_{d1(2)}^2\right)^{3/2}} \times \left(ik\sqrt{s_{1(2)}^2+s_3'^2+x_{d1(2)}^2}+1\right) \right] \mathrm{d}s'_3 \right\} \mathrm{d}s_{1(2)},$$

$$Z_{31(2)} = ix_{d1(2)} \int_{-L_3}^{L_3} f_3(s_3) \left\{ \int_{-L_{1(2)}}^{L_{1(2)}} f_{1(2)}\left(s'_{1(2)}\right) \left[\frac{e^{-ik\sqrt{s_3^2+s_{1(2)}'^2+x_{d1(2)}^2}}}{\left(s_3^2+s_{1(2)}'^2+x_{d1(2)}^2\right)^{3/2}} \times \left(ik\sqrt{s_3^2+s_{1(2)}'^2+x_{d1(2)}^2}+1\right) \right] \mathrm{d}s'_{1(2)} \right\} \mathrm{d}s_3,$$

The expressions $Z_{33}^{s(a)\Sigma} = Z_{33}^{s(a)Wg} + Z_{33}^{s(a)Hs}$ and $F_k^{s(a)}$ analogues to that defined in Section 3 can be used after replacing index sl by 33.

Thus, the equation system for the Clavin element on the waveguide can be written as

$$\begin{cases} J_{0v}Z_v^\Sigma - J_{0v}Z_{vv} + J_{0sl}^s Z_c = 0, \\ J_{0sl}^s Z_{sl}^{s\Sigma} - J_{0v}Z_c = -\dfrac{i\omega}{2k}H_{sl}^s, \\ J_{0sl}^a Z_{sl}^{a\Sigma} = -\dfrac{i\omega}{2k}H_{sl}^a. \end{cases} \tag{21}$$

The complex current amplitudes obtained by solving the equation system (21) are presented as:

$$\begin{aligned} J_{0v1} &= -\frac{i\omega}{2k}H_{sl}^s \frac{Z_c}{Z_{sl}^{s\Sigma}\left(Z_v^\Sigma - Z_{vv}\right) - Z_c^2}, \quad J_{0v2} = -J_{0v1}, \\ J_{0sl}^s &= -\frac{i\omega}{2k}H_{sl}^s \frac{Z_v^\Sigma - Z_{vv}}{Z_{sl}^{s\Sigma}\left(Z_v^\Sigma - Z_{vv}\right) - Z_c^2}, \quad J_{0sl}^a = -\frac{i\omega}{2k}H_{sl}^a \frac{1}{Z_{sl}^{a\Sigma}}. \end{aligned} \tag{22}$$

The current distribution along the vibrators and slot can be determined by the following expressions:

$$J_v(s) = \frac{i\omega}{2k^2}H_0 \cos\frac{\pi x_0}{a} J_v f_v(s), \quad J_{sl}(s) = -\frac{i\omega}{2k^2}H_0 \cos\frac{\pi x_0}{a}\left[J_{sl}^s f_{sl}^s(s) + iJ_{sl}^a f_{sl}^a(s)\right], \tag{23}$$

where $J_v = \frac{Z_c F_k^s}{Z_{sl}^{s\Sigma}(Z_v^\Sigma + Z_{vv}) + Z_c^2}$, $J_{sl}^s = \frac{(Z_v^\Sigma + Z_{vv})F_k^s}{Z_{sl}^{s\Sigma}(Z_v^\Sigma + Z_{vv}) + Z_c^2}$, $J_{sl}^a = -\frac{F_k^a}{Z_{sl}^{a\Sigma}}$.

All coefficients defined in Section 3 and the energy characteristics for this structure are defined by expressions (17)–(19) after replacing index 33 by index sl.

5. NUMERICAL AND EXPERIMENTAL RESULTS

The combined Clavin radiator consists of two identical perfectly conducting monopoles located on the plane screen symmetrically to the slot axis [21]. Clavin et al. have shown experimentally that RPs in the H-plane ($\varphi = 0^\circ$) and E-planes ($\varphi = 90^\circ$) are approximately identical if the monopoles with length $L_v = 0.375\lambda$ are placed symmetrical to the slot axis at distances $x_d = 0.086\lambda$. It is quite clear that according to expression (12), the RP in the H-plane has only the E_φ component, which coincides with the RP of stand-along slot since the monopole currents with equal amplitudes are in anti-phase relative to each other. The RP in the plane $\varphi = 0^\circ$ for the configuration with radiators placed over the infinite screen is shown in Fig. 4(a) and marked by a solid curve. According to Eq. (12), the RP in the E-plane has only the E_θ component, and its shape can be made closer to the H-plane RP shape by varying the vibrator currents. The RP for this case is shown in Fig. 4(a) by the dashed curve 1. Some improvement in the coincidence of the RP of the radiator in two planes in comparison with that observed in Fig. 4(a) in [21] was achieved due to the use of L-shaped vibrators.

The external problem solution by using trigonometric approximations for the slot and vibrator currents [23] have allowed to obtain the radiator parameters $L_v = 0.365\lambda$, $x_d = 0.065\lambda$ which are a little

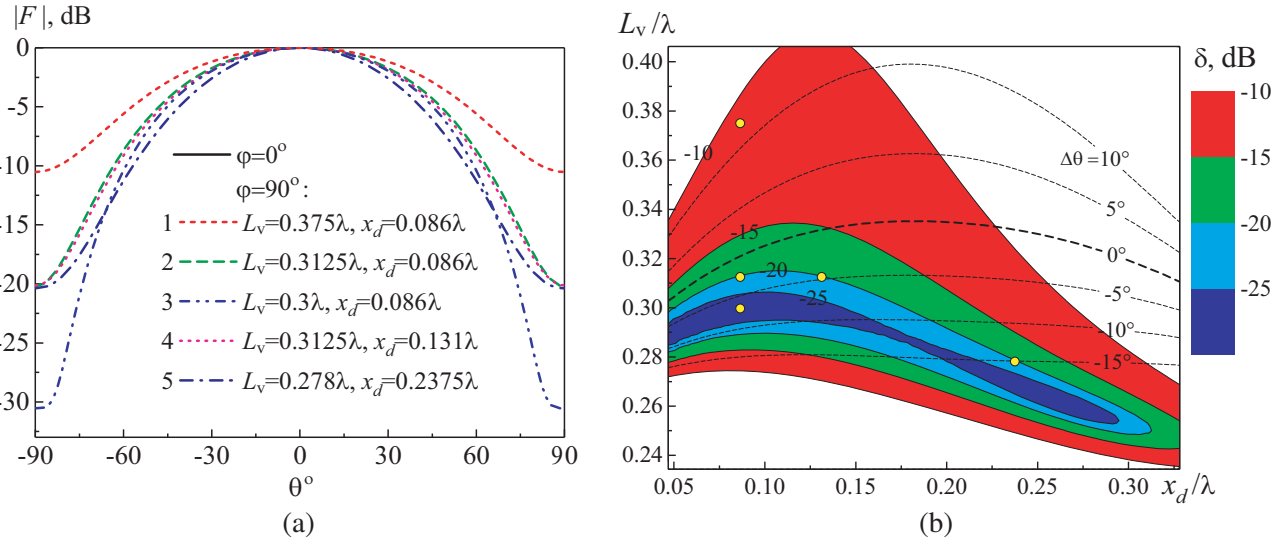

Figure 4. Characteristics of the Clavin radiator: (a) RPs obtained for various L_v and x_d; (b) the level of lateral radiation δ and difference between the RP widths in E- and H-plane $\Delta\theta$ as functions of L_v/λ and x_d/λ.

bit different from that obtained by Clavin et al. [21, 22]. This was achieved due to the lower radiation level along the plane than that in [21]. The simulation results have also shown that other pairs of parameters L_v/λ and x_d/λ can be selected for which RPs differ in shapes, but have the same level of lateral radiation. This can be seen from curves 2 and 5 in Fig. 4(a). In this regard, these results cannot claim to be complete, and further studies are required.

The influence of parameters L_v/λ and $2x_d/\lambda$ on the directivity characteristics of the Clavin type radiators is studied by computing the difference $\Delta\theta$ between the RP widths in E- and H-planes at -3 dB level and the level of lateral radiation δ, i.e., the maximum of E-plane RP.

The plots of δ and $\Delta\theta$ as functions of x_d/λ and L_v/λ are shown Fig. 4(b) where δ and $\Delta\theta$ are represented by the color scale level and level curves. The simulation results presented in Fig. 4(b) make it possible to conclude that there exist two options to obtain RPs with almost equal RP widths in the E and H planes. These options presented in Fig. 4(a) by curves 2 and 3 allow us to obtain RPs with a minimum level of side lobes equal to -20 dB ($L_v = 0.3125\lambda$, $x_d = 0.086\lambda$, curve 2) or with a low level of side radiation $\delta = -31$ dB ($L_v = 0.3\lambda$, $x_d = 0.086\lambda$, curve 3). Parameters L_v and x_d for the curves in Fig. 4(a) are marked in Fig. 4(b) by circles.

The energy characteristics of radiator were obtained with following parameters: $\lambda = 32$ mm, $a \times b = 23 \times 10$ mm^2, $h = 1$ mm, $2L_s = 16$ mm ($2L_s = 0.5\lambda$), $d = 1.5$ mm, $x_0 = 2.5$ mm, $r = 0.17$ mm. Since the ratios $2r_v/L_v$ and $[d/(2L_s)]$ do not exceed 0.1, the thin wire and narrow slot approximations were used during simulation. The energy characteristics of the combined Clavin radiators, whose RPs are presented in Fig. 4(a), are summarized in Table 1.

Table 1. The energy characteristics of combine Clavin radiators.

Geometric parameters	$\lvert S_{11}\rvert$	$\lvert S_{12}\rvert$	$\lvert S_{\Sigma}\rvert^2$	D
$L_v = 0.375\lambda$, $x_d = 0.086\lambda$	0.251	0.854	0.157	6.366
$L_v = 0.3125\lambda$, $x_d = 0.086\lambda$	0.207		0.074	7.485
$L_v = 0.3\lambda$, $x_d = 0.086\lambda$	0.184		0.057	7.854

The simulation results are presented in Fig. 5, where the radiation and reflection coefficients, directivity factor (D), and the gain (G) of the combined radiator are shown as the function of monopole electric length and the distance between the slot and monopole. These plots allow us to obtain the

required energy characteristics and directivity factor by selecting the geometric parameters of the radiator. The characteristic pairs of parameters are marked in Fig. 4(b) by circles.

It turned out that the lowest level of lateral radiation ($\delta = -31$ dB) for the radiator with the geometric parameters ($L_v = 0.3\lambda$, $x_d = 0.086\lambda$) can be obtained if radiation coefficient is rather low. This can be explained by the phasing conditions for the radiation fields of the slot and vibrators. Really, for full compensation of the radiation field of the slot along the plane in the far zone, a pair of vibrators should induce an equivalent electric field in the geometric center of the slot, equal in amplitude to the field of the slot and anti-phased one. Consequently, the compensation of intrinsic slot field can significantly reduce the radiating capacity of the slot. As from Fig. 5(b), the $|S_\Sigma|^2$ level increases if the distance between the vibrators is increased. This inevitable violates the phase relations and reduces the level of lateral radiation. As an example, consider the RP of the combined radiator with geometric parameters $L_v = 0.3\lambda$, $x_d = 0.131\lambda$, presented in Fig. 4(a) (curve 4). Comparing curves 1 and 4 shows that the radiation coefficient increases up to $|S_\Sigma|^2 = 0.184$ while the difference between the RPs' widths decreases ($\Delta\theta = -5°$). If the distance between the vibrators is further increased under conditions that $\delta = -20$ dB, the radiation and reflection coefficients become relatively large, $|S_\Sigma|^2 = 0.403$, $|S_{11}| = 0.525$. The directivity factor also increases ($D = 8.273$), and $\Delta\theta = -15°$ (curve 5 in Fig. 4(a)).

The analysis of the plots in Fig. 5 shows that the energy characteristics of the combined radiator can

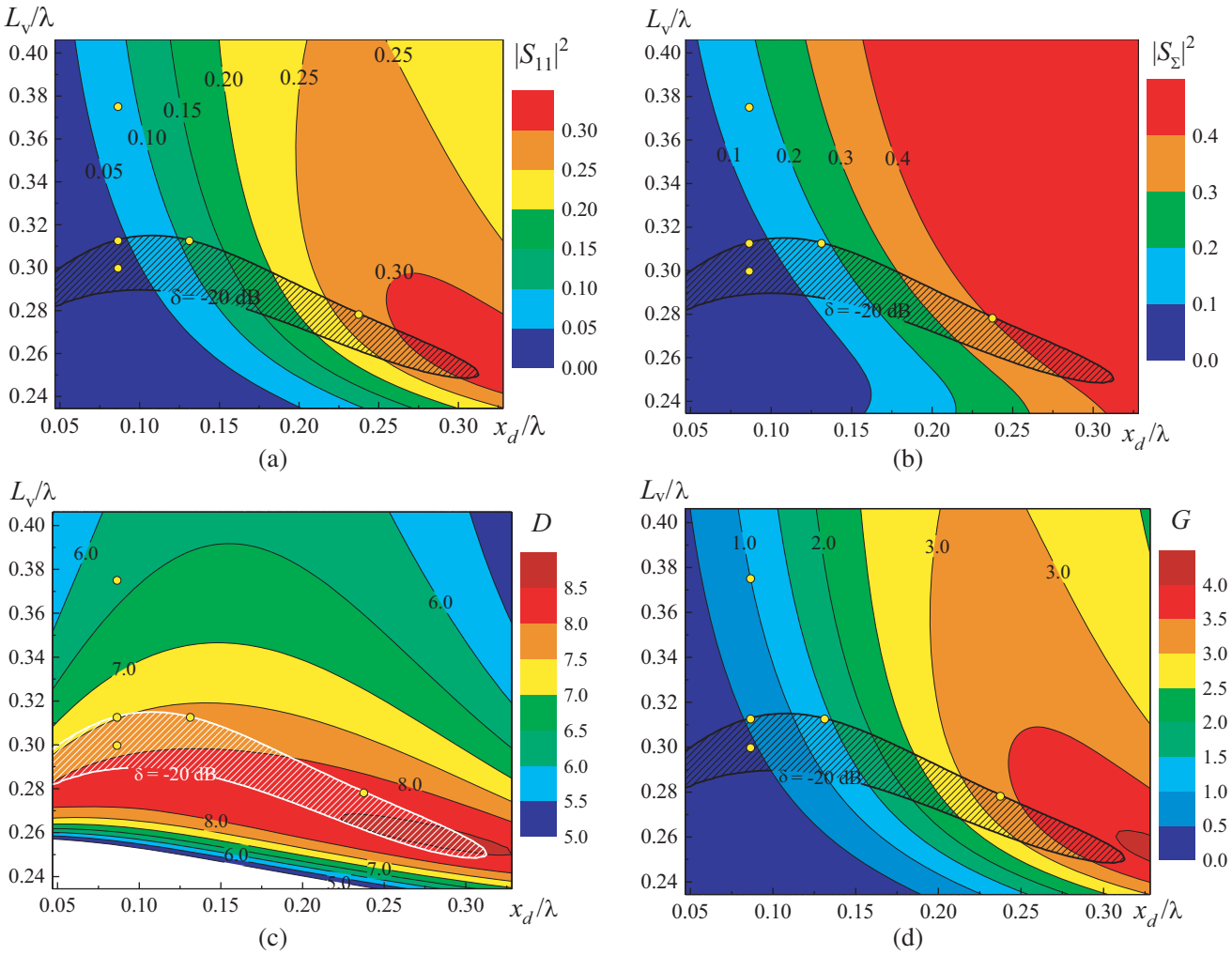

Figure 5. The energy characteristics of the combined radiator as functions of the electric monopole length and distance between the slot and vibrator: (a) $|S_{11}|$, (b) $|S_\Sigma|^2$, (c) D, and (d) G.

be controlled by varying the electric length of the vibrators. As known [4], the vibrator electric length can be varied by coating its surface with constant imaginary impedance. In this case, it can be assumed that the RP shape will not be substantially varied, since the RP of monopoles with electric lengths in the range $0 < L_v/\lambda < 0.3$ is similar to that of a perfectly conducting radiator. This assumption for the vibrator with constant impedance distribution can be verified for one a priori chosen impedance value.

The numerical results have shown that monopoles with inductive surface impedance make it possible to obtain specified radiator characteristics with shorter monopoles. For example, the electric length of the monopole with constant impedance $\bar{Z}_S = 0.1i$ can be reduced relative to their physical length by about 30%. The characteristics of the Clavin radiators are presented in Fig. 6 and Fig. 7. As can be seen, the parameter $\Delta\theta$ minimum and predefined level of lateral radiation δ can be obtained by varying the monopole length and distance between the slot and vibrators. The energy characteristic $|S_{11}|$, $|S_\Sigma|^2$, Da, and RP parameters δ and $\Delta\theta$ for the curves in Fig. 6(a) are presented in Table 2.

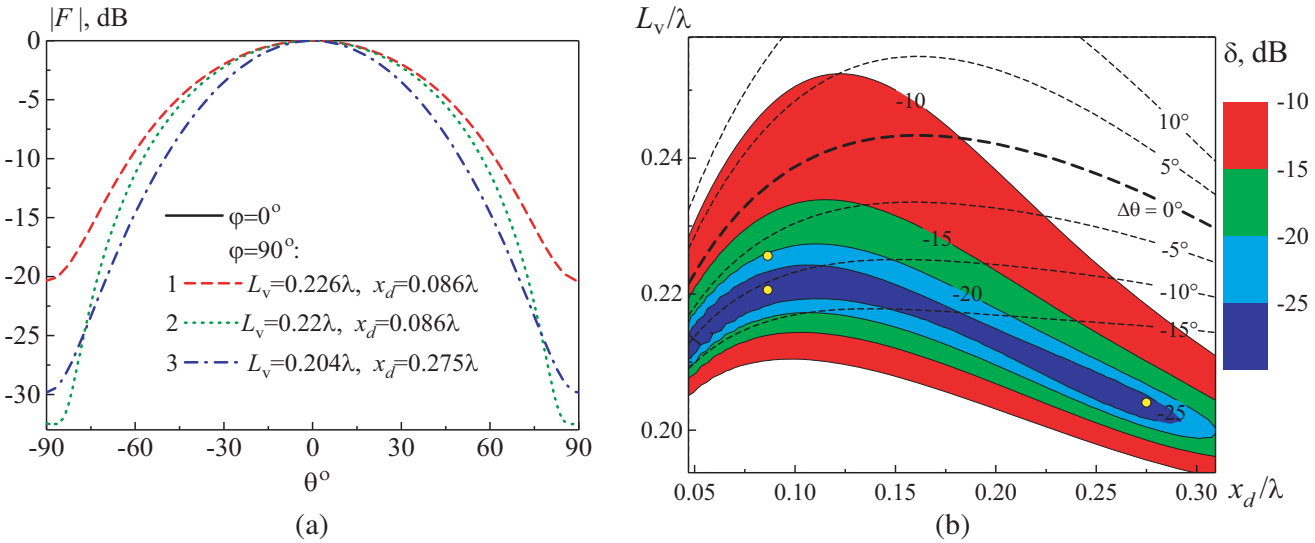

Figure 6. Characteristics of the Clavin radiator with impedance monopoles ($\bar{Z}_S = 0.1i$): (a) RP; (b) the level of lateral radiation δ and difference between the RP widths in E- and H-planes $\Delta\theta$ as functions of L_v/λ and x_d/la.

Table 2. The RP parameters and energy characteristics of the Clavin radiator with impedance monopoles.

δ, dB	$\Delta\theta$,	$\lvert S_{11}\rvert$	$\lvert S_\Sigma\rvert^2$	D	Curve in Fig. 6(a), No.
−20	−7	0.17	0.05	7.74	1
−32.5	−11.3	0.15	0.04	8.1	2

As can be seen from Fig. 7, when the distance between the vibrators is increased, and the length of the monopoles is decreased; the radiation coefficient D and, hence, the gain G are increased. At the same time, as can be seen from curve 3 in Fig. 6(a), parameter $\Delta\theta$ increases to $\Delta\theta = -23.7°$. Thus, the reflection and radiation coefficients can be varied over a wide range with the low lateral radiation level by fitting the length of the vibrators, distance between them, and/or their surface impedance.

It is quite clear that phase relationships for the fields in the combined waveguide radiator depend not only upon the vibrator geometry, but also upon the slot length, since when it deviates from resonant dimension, the slot intrinsic field becomes asymmetric due to longitudinal slot excitation. The simulation results have shown that the radiation coefficient can be increased by slight increasing the slot length relative to 0.5λ. The energy characteristics and directivity of the combine radiator with parameters: $\lambda = 32\,\text{mm}$, $a \times b = 23 \times 10\,\text{mm}^2$, $h = 1\,\text{mm}$, $d = 1\,\text{mm}$, $x_0 = a/4$, $r = 0.17\,\text{mm}$, $x_d = 0.086\lambda$ for perfectly conducting and impedance ($\bar{Z}_S = 0.1i$) vibrators placed on the waveguide. The RPs and

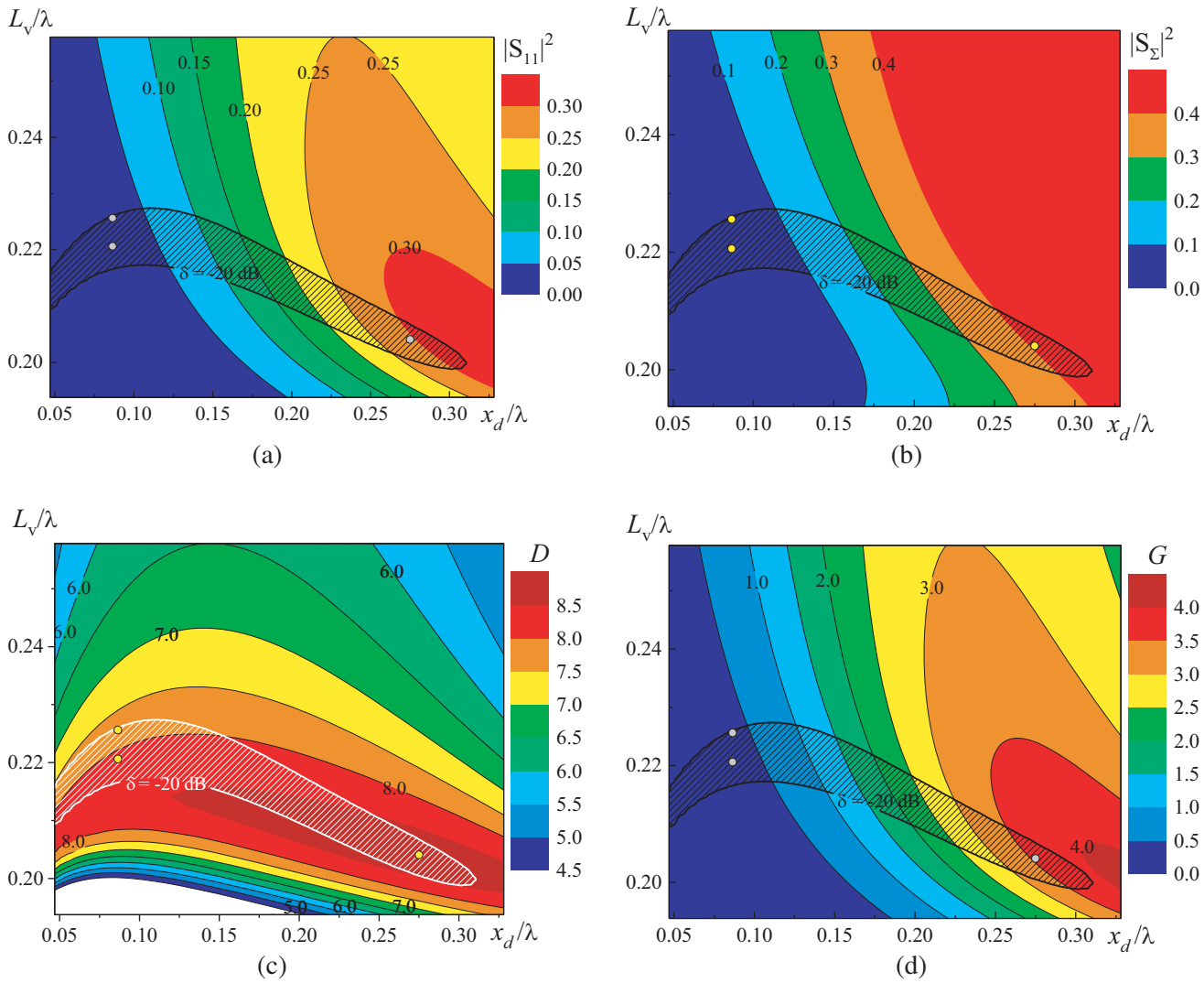

Figure 7. Characteristic of the Clavin radiator located on the waveguide with impedance vibrator ($\bar{Z}_S = 0.1i$): (a) reflection coefficient $|S_{11}|$, (b) radiation coefficient $|S_\Sigma|^2$, (c) directivity D, (d) gain G as function of L_v/λ and x_d/λ.

energy characteristics as function of the electric length of the slot and vibrators plotted by using the above parameters are shown in Figs. 8–11. Thus, the RPs of equal width in the E- and H-planes with the lateral radiation level $\delta = -20\,\text{dB}$ can be obtained if the perfectly conducting monopoles are used with parameters $L_v = 0.3\lambda$, $2L_s = 0.57\lambda$ (curve 1 in Fig. 11(a)). The RP closest in width ($\Delta\theta = -3.4^\circ$) can be obtained if the impedance monopoles with parameters $L_v = 0.22\lambda$, $2L_s = 0.57\lambda$ are used (curve 1 in Fig. 11(b)). The radiation coefficients obtained with these parameters are equal to $|S_\Sigma|^2 = 0.493$, $|S_\Sigma|^2 = 0.497$. The RPs with the lowest levels of lateral radiation, maximal radiation coefficient $|S_\Sigma|^2$, and the highest gain are presented in curve 2 and curve 3 of Fig. 11. The parameters L_v/λ and $2L_s/\lambda$ used for simulation are marked in Fig. 8 by circles.

All the curves presented above were plotted by using the parameters normalized at free space wavelength. This ensures simple evaluation of the radiator characteristics at the operating wavelength. The reliability of the proposed mathematical model for the combine radiator was confirmed by comparison with experimental data and the results found in literature. For example, the plots of the simulated and experimental reflection coefficients as functions of relative wavelength λ/λ_0 (λ_0 is wavelength in free space) for the single slot are presented in Fig. 12.

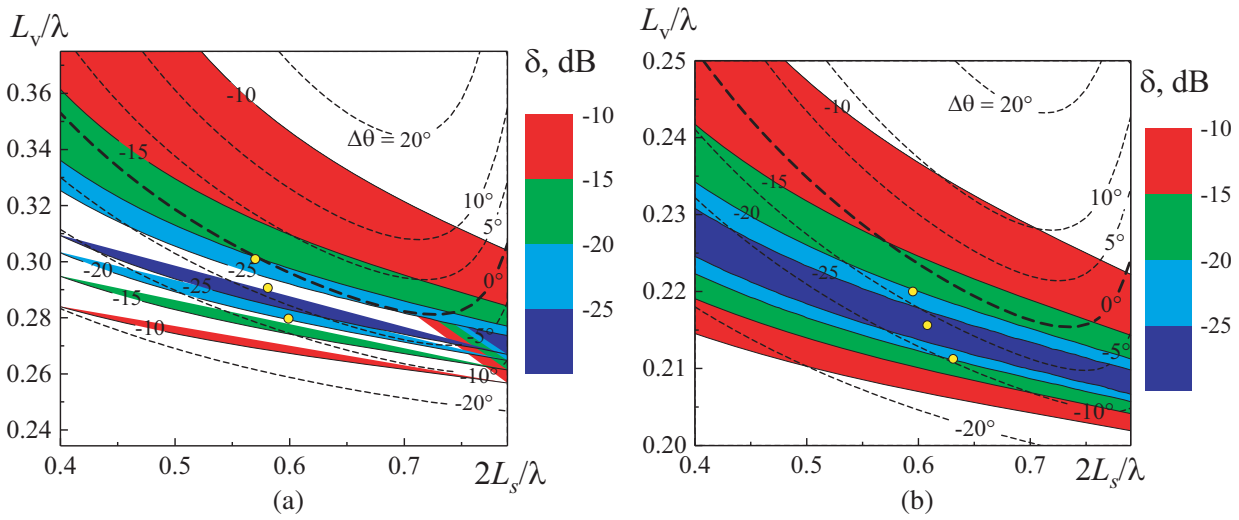

Figure 8. The level of lateral radiation δ and the RP width difference in orthogonal planes $\Delta\theta$ (dashed curves) as the function of L_v/λ and $x_d\lambda$: (a) $\bar{Z}_S = 0$, (b) $\bar{Z}_S = 0.1i$.

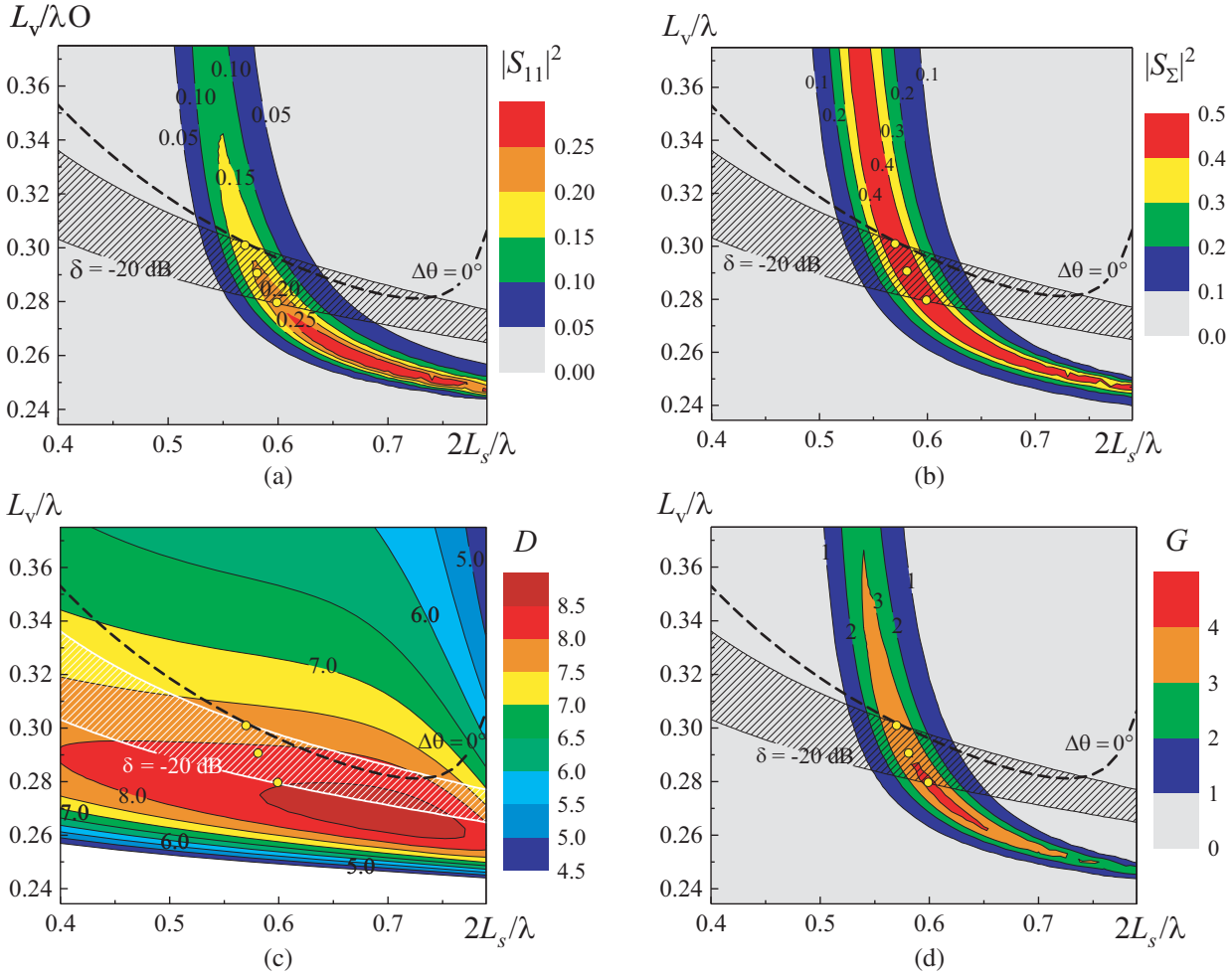

Figure 9. Energy characteristics of the Clavin radiator with perfectly conducting monopoles ($\bar{Z}_S = 0$) as function of L_v/λ and x_d/λ: (a) reflection coefficient $|S_{11}|$, (b) radiation coefficient $|S_\Sigma|^2$, (c) directivity D, (d) gain G.

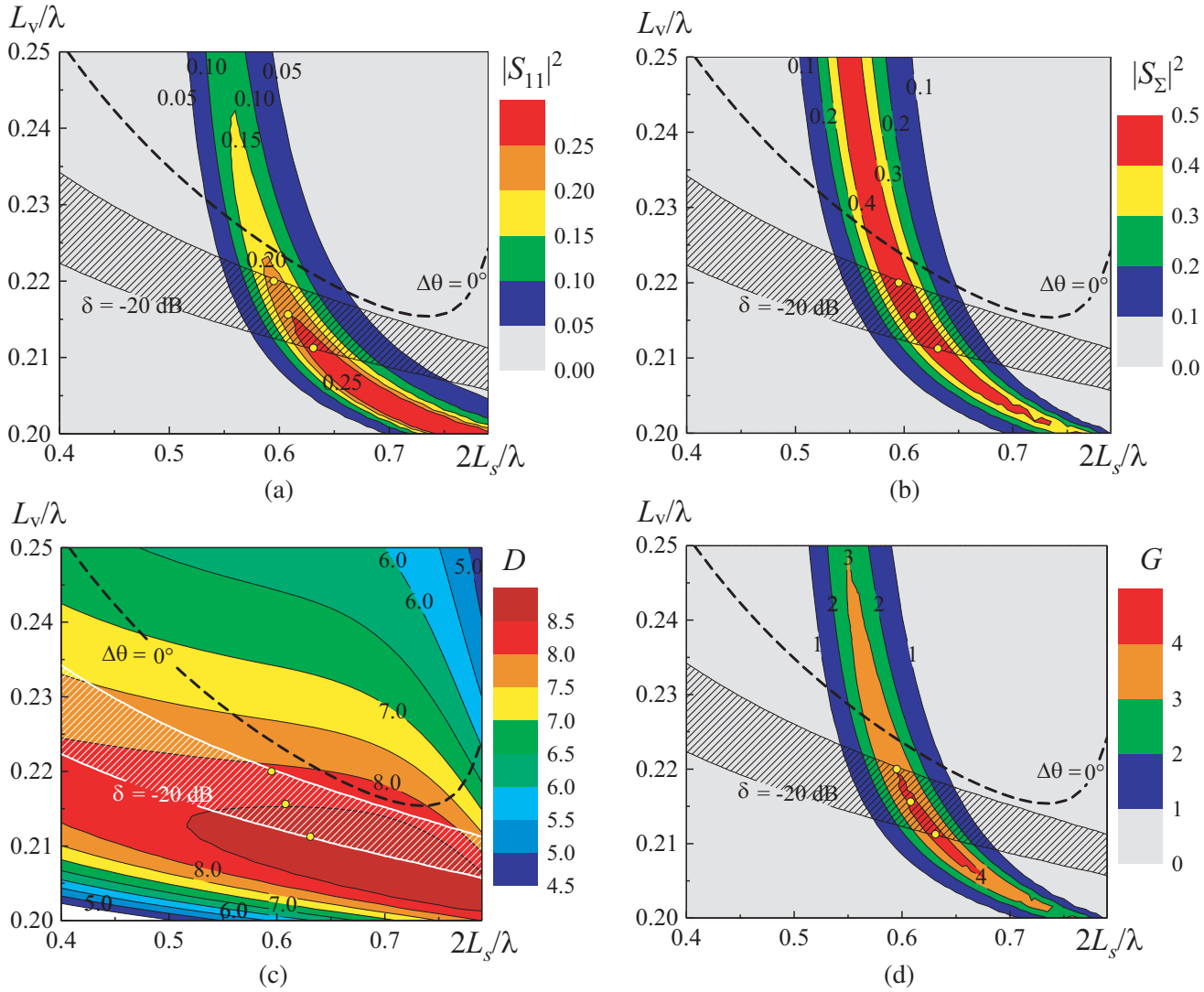

Figure 10. Energy characteristics of the combined radiator with impedance monopoles ($\bar{Z}_S = 0.1i$) as function of L_v/λ and x_d/λ: (a) reflection coefficient $|S_{11}|$, (b) radiation coefficient $|S_\Sigma|^2$, (c) directivity D, (d) gain G.

6. NUMERICAL RESULTS FOR THE COMBINED RADIATOR WITH THE TUNING MONOPOLE IN THE WAVEGUIDE

The energy coefficients of the Clavin radiator placed near the longitudinal slot cut in the broad wall of rectangular waveguide with the vibrator inside the waveguide are plotted as a function of the monopole parameters x_{0v}, L_V, presented in Fig. 13. The tuning vibrator is located in the plane $\{x0y\}$ inside the waveguide parallel to its narrow walls as shown in Fig. 1. The parameters of the radiator are as follows: $a \times b = 23 \times 10\,\text{mm}^2$, $h = 1\,\text{mm}$, $\lambda = 32\,\text{mm}$, $2L_s = 16\,\text{mm}$, $d = 1.5\,\text{mm}$, $x_0 = 2.5\,\text{mm}$, $r = 0.17\,\text{mm}$, $L_v = 0.3125\lambda\,\text{mm}$, $x_d = 0.086\lambda\,\text{mm}$. The radius and surface impedance of the monopole located in the waveguide are $r_V = 0.25\,\text{mm}$ and $\bar{Z}_{SV} = 0$.

As shown in the previous section, the optimal RP with equal width in the E- and H-planes can be formed by the radiating structure without tuning vibrator at $\lambda = 32\,\text{mm}$. This structure is characterized by the low radiation coefficient, $|S_\Sigma|^2 = 0.074$, and sufficiently high reflection coefficient. If the monopole is placed inside the waveguide, this relationship between the energy characteristic can be changed by fitting the monopole length L_V and its displacement x_{0v} relative to the waveguide wall.

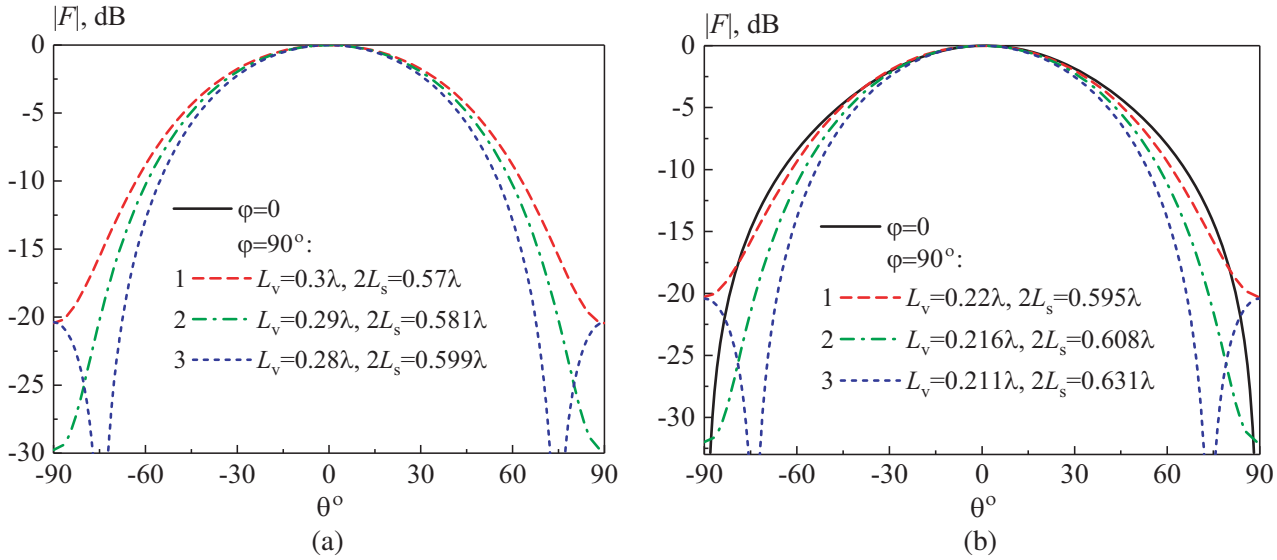

Figure 11. The RP of the Clavin radiator located on the waveguide in the main polarization planes as function of the angle θ for $\varphi = 0°$ and $\varphi = 90°$: (a) perfectly conducting vibrator, $\bar{Z}_S = 0$, (b) impedance vibrators, $\bar{Z}_S = 0.1i$.

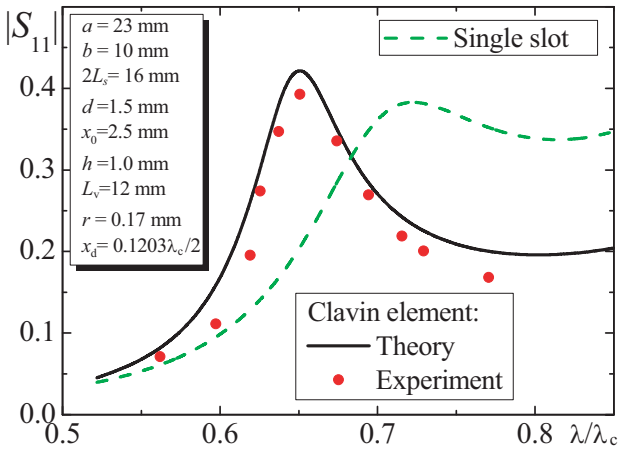

Figure 12. Dependence of the reflection coefficient for the combine radiator on the ratio λ/λ_c (λ_c is critical wavelength of the waveguide).

The simulation results have shown that the passive monopole weakly influences the slot, since the monopole is placed directly in the region under the slot aperture. This effect can be explained by the general electrodynamic property of thin vibrators, i.e., by the absence of radiation (scattering) in the direction of their longitudinal axes. Furthermore, the longer the monopole is, the smaller its influence is on the slot. As can be seen from Fig. 13, if the monopole length is $L_V = 8.5\,\text{mm}$, and the displacement x_{0v} varies in the range $1.75\,\text{mm} \leq x_{0v} \leq 3.25\,\text{mm}$, the transmission coefficient $|S_{12}|$ decreases at about 5%. However, the internal monopole improves the radiator matching with the waveguide by almost 10 times. This effect is important for using combined radiators in multi-element linear antenna arrays with dimensions of the order of hundreds λ. Such an array, for example, can be used on spacecrafts.

The spatial separation of the slot and the monopole inside the waveguide can significantly increase the radiation coefficient, while the directional characteristics of the combined radiator are not varied. For example, if the monopole with parameters $L_V = 7.2\,\text{mm}$, $x_{0v} = 17.5\,\text{mm}$ is used, the radiation coefficient increases up to $|S_\Sigma|^2 = 0.4$ (Fig. 13). Thus, the additional inhomogeneity in the waveguide

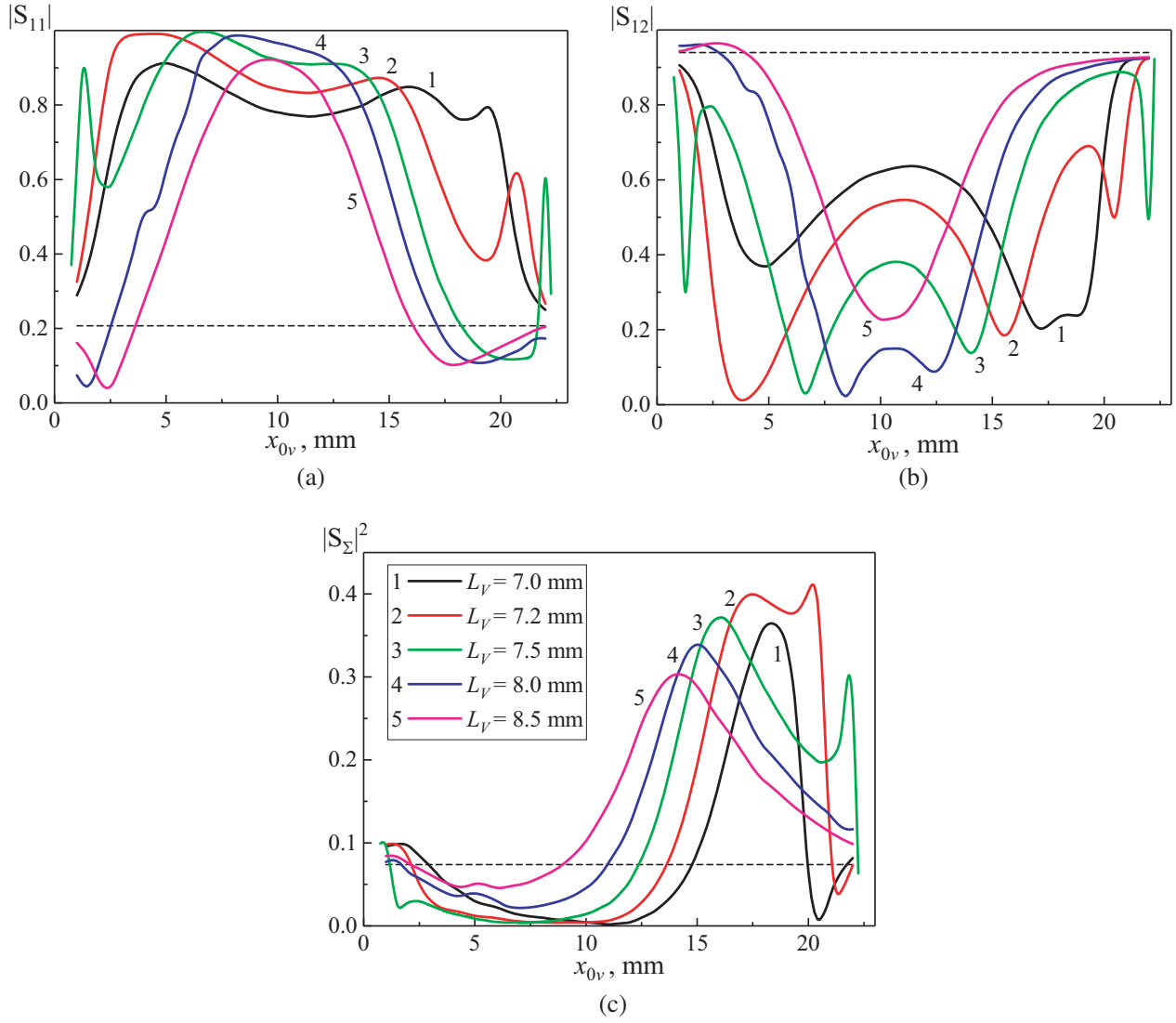

Figure 13. The energy characteristic of the combined radiator with tuning vibrator as functions of the monopole location x_{0v} for various monopole lengths L_V: (a) reflection $|S_{11}|$, (b) transmission coefficient $|S_{12}|$, (c) radiation coefficient $|S_\Sigma|^2$. The coefficients for the waveguide without tuning vibrator are shown in the plots by dashed lines.

in the form of the monopole increases the reflection coefficient relative to the stand-along resonant slot to $|S_{11}| = 0.55$.

7. CONCLUSION

In this article, the mathematical model of a combined waveguide structure with the Clavin type radiator is constructed based on the solution of the diffraction problem in a strict formulation by the generalized method of induced EMMF. In contrast to the publications of other authors known in the literature, vibrator elements in the form of impedance monopoles are considered for the first time. The influence of the vibrator lengths and the distance between the vibrators on the directional characteristics of the combined radiator were analyzed to obtain the optimal level of lateral radiation in the E-plane and the difference in the RP widths in E- and H-planes at the level of -3 dB. It was shown that the directivity and energy characteristics of the combined radiator: the RP form, radiation and reflection coefficients,

directivity factor and gain can be controlled in a wide range by varying the electric vibrator length, distance between the vibrators, and their surface reactive impedances. It was shown that the combined radiators with optimal characteristics can be realized by using shorter vibrators with inductive surface impedance than perfectly conducting vibrator. It was found that the slot radiation coefficient can be increased by increasing the slot length by 15–20% relative to its resonance length, while the RPs in the E and H planes do not vary. The simulation results have confirmed the possibility to effectively control the energy characteristics of the combined radiator by using the tuning monopole in the waveguide. Since the multi-parameter resonant tuning of the radiator is difficult to achieve experimentally, this is a separate problem requiring further studies. The results obtained can be useful in the design of stand-alone waveguide radiator and multi-element waveguide arrays, with combined radiators based on the Clavin elements, including devices with non-mechanical controlling the electrodynamic characteristics.

REFERENCES

1. Nesterenko, M. V., V. A. Katrich, Yu. M. Penkin, and S. L. Berdnik, *Analytical and Hybrid Methods in Theory of Slot-Hole Coupling of Electrodynamic Volumes*, Springer Science+Business Media, New York, 2008.
2. Balanis, C. A. (ed.), *Modern Antenna Handbook*, John Wiley & Sons, Hoboken, 2008.
3. Penkin, Yu. M., V. A. Katrich, M. V. Nesterenko, S. L. Berdnik, and V. M. Dakhov, *Electromagnetic Fields Excited in Volumes with Spherical Boundaries*, Springer Nature Swizerland AG, Cham, Swizerland, 2019.
4. Nesterenko, M. V., V. A. Katrich, Yu. M. Penkin, V. M. Dakhov, and S. L. Berdnik, *Thin Impedance Vibrators. Theory and Applications*, Springer Science+Business Media, New York, 2011.
5. King, R. W. P. and G. H. Owyang, "The slot antenna with coupled dipoles," *IRE Trans. Antennas Propag.*, Vol. 8, 136–143, 1960.
6. Butler, C. M. and K. R. Umashankar, "Electromagnetic excitation of a wire through an aperture-perforated conducting screen," *IEEE Trans. Antennas Propag.*, Vol. 24, 456–462, 1976.
7. Naiheng, Y. and R. Harrington, "Electromagnetic coupling to an infinite wire through a slot in a conducting plane," *IEEE Trans. Antennas Propag.*, Vol. 31, 310–316, 1983.
8. Halpern, B. M. and P. E. Mayes, "The monopole slot as a two-port diversity antenna for UHF land-mobile radio systems," *IEEE Trans. Vehicular Technology*, Vol. 33, 76–83, 1984.
9. His, S. W., R. F. Harrington, and J. R. Mautz, "Electromagnetic coupling to a conducting wire behind an aperture of arbitrary size and shape," *IEEE Trans. Antennas Propag.*, Vol. 33, 581–587, 1985.
10. Lee, Y.-H., D.-H. Hong, and J.-W. Ra, "Waveguide slot antenna with a coupled dipole above the slot," *Electronics Letters*, Vol. 19, 280–282, 1983.
11. Hirokawa, J., L. Manholm, and P.-S. Kildal, "Analysis of an untilted wire-excited slot in the narrow wall of a rectangular waveguide by including the actual external structure," *IEEE Trans. Antennas Propag.*, Vol. 45, 1038–1044, 1997.
12. Morioka, T., K. Komiyama, and K. Hirasawa, "Effects of a parasitic wire on coupling between two slot antennas," *IEICE Trans. Commun.*, Vol. E84-B, 2597–2603, 2001.
13. Wongsan, R., C. Phongcharoenpanich, M. Krairiksh, and J.-I. Takada, "Impedance characteristic analysis of an axial slot antenna on a sectoral cylindrical cavity excited by a probe using method of moments," *IEICE Trans. Fundament.*, Vol. E86-A, 1364–1373, 2003.
14. Park, S.-H., J. Hirokawa, and M. Ando, "Simple analysis of a slot and a reflection-canceling post in a rectangular waveguide using only the axial uniform currents on the post surface," *IEICE Trans. Commun.*, Vol. E86-B, 2482–2487, 2003.
15. Kim, K.-C., S. M. Lim, and M. S. Kim, "Reduction of electromagnetic penetration through narrow slots in conducting screen by two parallel wires," *IEICE Trans. Commun.*, Vol. E88-B, 1743–1745, 2005.
16. Lim, K.-S., V.-C. Koo, and T.-S. Lim, "Design, simulation and measurement of a post slot waveguide antenna," *J. of Electromagn. Waves and Appl.*, Vol. 21, No. 12, 1589–1603, 2007.

17. Nesterenko, M. V., V. A. Katrich, Y. M. Penkin, S. L. Berdnik, and V. I. Kijko, "Combined vibrator-slot structures in electrodynamic volumes," *Progress In Electromagnetics Research B*, Vol. 37, 237–256, 2012.
18. Nesterenko, M. V., V. A. Katrich, D. Y. Penkin, S. L. Berdnik, and V. I. Kijko, "Electromagnetic waves scattering and radiation by vibrator-slot structure in a rectangular waveguide," *Progress In Electromagnetics Research M*, Vol. 24, 69–84, 2012.
19. Penkin, D. Y., S. L. Berdnik, V. A. Katrich, M. V. Nesterenko, and V. I. Kijko, "Electromagnetic fields excitation by a multielement vibrator-slot structures in coupled electrodynamics volumes," *Progress In Electromagnetics Research B*, Vol. 49, 235–252, 2013.
20. Berdnik, S. L., V. A. Katrich, M. V. Nesterenko, Y. M. Penkin, and D. Y. Penkin, "Radiation and scattering of electromagnetic waves by a multi-element vibrator-slot structure in a rectangular waveguide," *IEEE Trans. Antennas Propag.*, Vol. 63, 4256–4259, 2015.
21. Clavin, A., D. A. Huebner, and F. J. Kilburg, "An improved element for use in array antennas," *IEEE Trans. Antennas Propag.*, Vol. 22, 521–526, 1974.
22. Clavin, A., "A multimode antenna having equal E- and H-planes," *IEEE Trans. Antennas Propag.*, Vol. 23, 735–737, 1975.
23. Papierz, A. B., S. M. Sanzgiri, and S. R. Laxpati, "Analysis of antenna structure with equal E- and H-plane patterns," *Proc. IEE.*, Vol. 124, 25–30, 1977.
24. Elliott, R. S., "On the mutual admittance between Clavin elements," *IEEE Trans. Antennas Propag.*, Vol. 28, 864–870, 1980.
25. Kominami, M. and K. Rokushima, "Analysis of an antenna composed of arbitrarily located slots and wires," *IEEE Trans. Antennas Propag.*, Vol. 32, 154–158, 1984.
26. Berdnik, S. L., V. A. Katrich, M. V. Nesterenko, Y. M. Penkin Yu. M., and S. V. Pshenichnaya, "Clavin element with impedance monopoles," *Proc. of the XX-th International Seminar/Workshop on Direct and Inverse Problems of Electromagnetic and Acoustic Wave Theory*, Lviv, Ukraine, 61–65, 2015.
27. Berdnik, S. L., N. K. Blinova, V. A. Katrich, M. V. Nesterenko, and Y. M. Penkin, "Spherical antenna with a Clavin radiator," *Proc. of the XX-th International Seminar/Workshop on Direct and Inverse Problems of Electromagnetic and Acoustic Wave Theory*, Lviv, Ukraine, 75–77, 2015.
28. Penkin, Yu. M., V. A. Katrich, and M. V. Nesterenko, "Two-frequency operating mode of antenna arrays with radiators of Clavin type and switching vibrator and slot elements," *Progress In Electromagnetics Research M*, Vol. 87, 171–178, 2019.
29. Nesterenko, M. V., S. L. Berdnik, V. A. Katrich, and Y. M. Penkin, "Electromagnetic waves excitation by thin impedance vibrators and narrow slots in electrodynamic volumes," Chapter in book *Advanced Electromagnetic Waves*, S. O. Bashir (ed.), Chapter 6, 147–176, Rijeka, InTech., 2015.